Differentiable Decision Tree via "ReLU+Argmin" Reformulation

Qiangqiang Mao, Jiayang Ren, Yixiu Wang, Chenxuanyin Zou, Jingjing Zheng, Yankai Cao[*]
University of British Columbia, Vancouver, Canada

Abstract

Decision tree, despite its unmatched interpretability and lightweight structure, faces two key issues that limit its broader applicability: non-differentiability and low testing accuracy. This study addresses these issues by developing a differentiable oblique tree that optimizes the entire tree using gradient-based optimization. We propose an exact reformulation of hard-split trees based on "ReLU+Argmin" mechanism, and then cast the reformulated tree training as an unconstrained optimization task. The ReLU-based sample branching, expressed as exact-zero or non-zero values, preserve a unique decision path, in contrast to soft decision trees with probabilistic routing. The subsequent Argmin operation identifies the unique zero-violation path, enabling deterministic predictions. For effective gradient flow, we approximate Argmin behaviors by scaling softmin function. To ameliorate numerical instability, we propose a warm-start annealing scheme that solves multiple optimization tasks with increasingly accurate approximations. This reformulation alongside distributed GPU parallelism offers strong scalability, supporting 12-depth tree even on million-scale datasets where most baselines fail. Extensive experiments demonstrate that our optimized tree achieves a superior testing accuracy against 14 baselines, including an average improvement of 7.54% over `CART`.

1 Introduction

Decision trees have attracted significant attention in machine learning primarily due to their interpretability and lightweight structures. Their strength lies in transparent "IF-THEN" rules, making them ideal for tasks requiring clear decision-making processes. However, their practical use is often limited by the lower test accuracy, forcing a shift towards other models that sacrifice interpretability advantages. Another limitation is the non-differentiability, which severely restricts their gradient-based applications, especially when embedded in optimization tasks. For instance, in reinforcement learning, decision trees offer an interpretable alternative to neural networks for policy representation; yet, non-differentiability remains a major barrier [Vos and Verwer, 2024, Marton et al., 2025].

Aiming for higher accuracy and fewer parameters, oblique decision tree, a pivot extension of classic orthogonal tree, holds great potential. Oblique tree uses linear feature combination for hyperplane splits. When data distribution follows hyperplane boundaries, it tends to generate smaller trees with higher accuracy [Costa and Pedreira, 2023]. Nevertheless, inducing oblique trees is challenging, owing to innumerable linear combinations at each node [Zhu et al., 2020]. Earlier works focus on optimizing splits at an individual node using greedy algorithms like `CART-LC` [Breiman et al., 1984] and `OC1` [Murthy et al., 1994]. Alternative methods rely on greedy orthogonal `CART` to induce oblique trees by rotating feature space, exemplified by `HHCART` [Wickramarachchi et al., 2015] and `RandCART` [Blaser and Fryzlewicz, 2016]. Despite their advancements, such greedy methods may be suboptimal due to weaker splits at subsequent nodes. To avoid this, non-greedy approach `TAO` [Zharmagambetov and Carreira-Perpinan, 2020] optimizes a subset of nodes at each step. Considering optimizing all

[*]Corresponding author: yankai.cao@ubc.ca.

nodes, Bertsimas and Dunn [2017] presents optimal tree to formulate tree training as a mixed-integer programming (MIP). Besides, sparse optimal trees [Lin et al., 2022] complements MIP-based work by considering sparsity. However, these methods often face scalability issues, especially for oblique tree with expanded search space. Recent efforts in optimal oblique tree [Boutilier et al., 2023, Zhu et al., 2020] have been confined to classification tasks with limited categorical predictions. In contrast, regression tasks with infinite continuous outputs remain challenging. In response, the originators of MIP-based work propose a local search alternative `ORT-LS` [Dunn, 2018] for tasks that are unsolvable by MIP. However, `ORT-LS` still suffers from high computational cost and suboptimal accuracy.

To significantly improve computational tractability compared to those MIP formulations, in this work, we reformulate entire tree training as an unconstrained optimization task. Our reformulation makes it easily solvable via gradient-based tools and also facilitates adapting it into a differentiable tree. The classic tree's non-differentiability mainly arises from two sources of hard decisions: hard splits at branch nodes that determine sample branching, and the unique decision path that assign each sample to a specific leaf node for sample prediction. Given the non-differentiability of hard decisions, two intuitive solutions have been used: treating the gradient via straight-through estimators (STE) like `DGT` [Karthikeyan et al., 2022], `GradTree` [Marton et al., 2023] and `DTSemNet` regression tree [Panda et al., 2024], and approximating binary decisions (0 or 1) with continuous probabilities in (0,1) using soft approximations like sigmoid function in soft trees [İrsoy et al., 2012, Wan et al., 2021, Frosst and Hinton, 2017] and other soft variants like smooth-step functions in `TEL` [Hazimeh et al., 2020]. However, STE may neglect critical gradient information, resulting in suboptimal learning, as evidenced by results reported in the original work of [Marton et al., 2023], where their method underperforms `CART` on 17 of 36 datasets (their Tables 1 and 2), as well as in our own experiments. Regarding soft approximations, previous efforts predominantly construct "soft" decision trees with soft splits, probabilistic path and predictions. Nonetheless, there do exist scenarios where a hard split or decision is not only appropriate but also imperative, as in Appendix A. Besides, other gradient-based trees exist, but they might not preserve classic tree structures or be exact reformulations, such as `DNDT` [Yang et al., 2018] which uses Kronecker products for class predictions, and the method by Norouzi et al. [2015] which uses a surrogate loss. Due to their differences in structure, formulation and optimization, we consider them complementary work suited for distinct application scenarios.

To retain the two sources of hard decisions, we propose a "ReLU+Argmin"-based exact reformulation. ReLU functions enforce hard decisions to direct samples left or right, and quantify violations of the correct directions that a sample must follow to reach its unique leaf. Our ReLU-based splits, in sharp contrast to soft splits with left-right probability, yield hard (exact-zero or non-zero) decisions for sample branching. This leverages ReLU's property of producing distinct zero and non-zero values at True-False decision boundaries. Such a property has ever been used to implicitly mimic a decision tree using neural networks [Lee and Jaakkola, 2020], in contrast to our direct application for reformulating and optimizing a tree. Next, the correct decision path is identified as the unique path with zero cumulative violations. This can be easily formulated via Argmin operation over zero and non-zero (positive) values. To avoid undefined gradient in Argmin, we approximate it with a scaled softmin function. Noticeably, two clarifications are necessary: first, our Argmin is a mathematical operation over a discrete set, and it should not be confused with "Argmin Differentiation" or "Implicit Differentiation" [Gould et al., 2016]. The latter is used in `LatenTree` [Zantedeschi et al., 2021], which frames tree training as a relaxed MIP problem within a bilevel optimization setting. However, their work is not directly related to our unconstrained task, and unrelated to approximate the Argmin operation itself. Second, our softmin approximation is introduced purely to facilitate gradient backpropagation during training; at the inference phase, our method reverts to using Argmin for deterministic behavior. This technique of using approximation during training while reverting to original function during inference was previously used in the work of [Mao and Cao, 2024].

Our Contributions: First, we propose a "ReLU+Argmin"-based exact reformulation for hard-split trees, avoiding softness introduced in sample branching and predictions. Second, we cast the entire tree training as an unconstrained optimization task, introducing a scaled softmin function to approximate Argmin behaviors for effective gradient flow. Third, to balance approximation degree with numerical instabilities, we present a strategy of multi-run warm start annealing to progressively refine solutions. Fourth, our implementation supports multi-GPU acceleration, significantly enhancing scalability. Finally, we provide an extensible "**R**eLU+**A**rgmin"-based **D**ifferentiable **D**ecision **T**ree optimization framework (termed `RADDT`) for inducing both regression trees and classification trees. The source code is available in `https://github.com/YankaiGroup/RADDT`.

Performance: Experiments mainly focus on regression tasks across 17 medium-scale datasets and 7 million-scale datasets, showing our competitive testing accuracy as well as strong scalability. To enable a more convincing comparison, additional evaluations on the same datasets used in the original work of certain compared baselines further highlight the superiority of our method.

- Our optimized trees outperform the compared decision trees in testing accuracy. Notably, it outperforms `CART` by 7.54%, local search `ORT-LS` by 3.72%, and gradient-based `LatentTree` by 6.24%, and `DGT` by 2.66% on average.
- Our trees with linear predictions impressively outperforms tree ensembles, including random forest by 2.01%, `XGBoost` by 1.12% and gradient-based `TEL` by 0.76%.
- Our method successfully scales to 12-depth deep tree on million-scale datasets, where existing gradient-based trees like `GradTree`, `SoftDt`, `DGT` and `LatentTree` fail.

2 Foundations of Oblique Decision Tree

We explore oblique decision trees from an optimization perspective by formulating tree training as an optimization problem for both regression and classification tasks. For ease of understanding, we follow the notation for optimal binary trees as used in the original work of Bertsimas and Dunn [2017]. Consider a dataset $\{\boldsymbol{x}_i, y_i\}_{i=1}^n$ with input $\boldsymbol{x}_i \in [0,1]^p$, and output values $y_i \in [0,1]$ for regression and $y_i \in \{1, \cdots, c\}$ for classification with c classes. A binary tree of depth D comprises $T = 2^{D+1} - 1$ nodes, where each node is indexed by $t \in \mathbb{T} = \{1, \cdots, T\}$ in a breadth-first order. The nodes can be categorized into two types: branch nodes, which execute branching tests and are denoted by $t \in \mathbb{T}_B = \{1, \cdots, \lfloor T/2 \rfloor\}$, and leaf nodes denoted by $t \in \mathbb{T}_L = \{\lfloor T/2 \rfloor + 1, \cdots, T\}$, responsible for leaf predictions. Each branch node comprises a split weight $\boldsymbol{a}_t \in \mathbb{R}^p$ and a split threshold $b_t \in \mathbb{R}$ to conduct a branching test ($\boldsymbol{a}_t^T \boldsymbol{x}_i \leq b_t$) for samples allocated to that particular branch node. If a sample $\boldsymbol{x}_i$ passes the branching test, it is directed to the left child node at index $2t$; otherwise, to the right at index $2t+1$. Each leaf node contains θ_t to provide a prediction value specific to the current leaf, which varies depending on the task. For classification, $\theta_t = \{h_t \in \mathbb{R}^c\}$, and the prediction for a sample $\boldsymbol{x}_i$ assigned to leaf t is $\hat{y_i} = h_t$. For regression, $\theta_t = \{\boldsymbol{k}_t \in \mathbb{R}^p, h_t \in \mathbb{R}\}$, which considers two types of leaf prediction: linear and constant prediction. Specifically, tree with linear predictions involves a linear feature combination [Quinlan, 1998], with a general form of $\hat{y_i} = \boldsymbol{k}_t^T \boldsymbol{x}_i + h_t$. Tree with constant predictions is a special case of linear predictions, where $\boldsymbol{K}$ remains zero. It is the most commonly used type in existing decision tree methods, with $\hat{y_i} = h_t$. The training of oblique trees involves solving the following optimization problem:

$$\min_{\boldsymbol{A}, \boldsymbol{b}, \theta} \ \ell\left(y_i, \hat{y_i}\right) \tag{1a}$$

$$\text{s.t. } \ \hat{y_i} = f_{tree}(\boldsymbol{A}, \boldsymbol{b}, \theta, \boldsymbol{x}_i), \ i \in \{1, \cdots, n\}, \tag{1b}$$

where f_{tree} is the decision tree model, $\ell(\cdot)$ is square error loss for regression and cross entropy loss for classification. $\boldsymbol{A} = \{\boldsymbol{a}_1, \cdots, \boldsymbol{a}_{\lfloor T/2 \rfloor}\}$ and $\boldsymbol{b} = \{b_1, \cdots, b_{\lfloor T/2 \rfloor}\}$ are tree split parameters, $\theta = \{\theta_{\lfloor T/2 \rfloor + 1}, \cdots, \theta_T\}$ is leaf prediction parameter.

3 Unconstrained Optimization Reformulation for Oblique Tree Training

We first propose an exact reformulation of decision trees and further cast the training as an unconstrained task, allowing for gradient-based optimization for improved solvability and accuracy.

3.1 "ReLU+Argmin"-based exact reformulation for hard-split decision trees

ReLU-based hard splits and correctly-directed path formulation (no softness at branch nodes for sample branching)**:** A sample $\boldsymbol{x}_i$ is correctly assigned to a leaf node t by following a sequence of left-right decisions at its ancestor nodes. The ancestor nodes set $\mathbb{A}_t$ consists of left $\mathbb{A}_t^l$ and right $\mathbb{A}_t^r$ ancestors, traversed via left and right branch, respectively, such that $\mathbb{A}_t = \mathbb{A}_t^l \cup \mathbb{A}_t^r$. For left ancestor node $j \in \mathbb{A}_t^l$, $\boldsymbol{x}_i$ must pass the branching test $\boldsymbol{a}_j^T \boldsymbol{x}_i \leq b_j$ to be directed to the left, whereas for right $j \in \mathbb{A}_t^r$, it must fail the test to proceed right. To formulate these left-right hard decisions for $\boldsymbol{x}_i$, we use ReLU functions to characterize the violation of correct direction at each node j, termed $v_{i,j}$:

$$v_{i,j} = \begin{cases} ReLU\left(\boldsymbol{a}_j^T \boldsymbol{x}_i - b_j\right), & j \in \mathbb{A}_t^l \\ ReLU\left(b_j - \boldsymbol{a}_j^T \boldsymbol{x}_i\right), & j \in \mathbb{A}_t^r, \end{cases} \tag{2}$$

where $v_{i,j} = 0$ indicates that $\boldsymbol{x}_i$ follows the correct direction, i.e. left for $\mathbb{A}_t^l$ and right for $\mathbb{A}_t^r$, while $v_{i,j} \neq 0$ is a violation of correct direction. These deterministic ReLU-based zero and non-zero values eliminate the softness in sample branching, as opposed to soft approximations with continuous probabilities in (0,1) at each branch node. The cumulative violations across all branch nodes are:

$$U_{i,t} = \sum_{j \in \mathbb{A}_t^l} v_{i,j} + \sum_{j \in \mathbb{A}_t^r} v_{i,j}, \tag{3}$$

where $U_{i,t} = 0$ indicates $\boldsymbol{x}_i$ follows all correct directions to leaf node t; otherwise $U_{i,t} \neq 0 (> 0)$ corresponds to the overall violations of correct sample assignments.

Unique decision path formulation using Argmin (no softness at leaf nodes for sample prediction)**:** Since x_i follows a unique decision path to a specific leaf node, only one leaf node holds a violation-free path. Such a unique zero $U_{i,t}$ removes the softness in sample assignment and prediction, in contrast to soft approximations with probabilistic paths for predictions. The unique path can be easily formulated by Argmin function (more concretely, one-hot encoded Argmin $\mathbb{M}$) applied to $U_{i,t}$:

$$\mathbb{M}\left(U_{i,t}\right) = \mathbb{1}\left(t = (\text{Argmin}(\mathbf{U}_i) + \lceil T/2 \rceil)\right), \tag{4}$$

where $\mathbf{U}_i = \{U_{i,\lfloor T/2 \rfloor + 1}, \cdots, U_{i,T}\}$. $\mathbb{M}(\cdot)$ is the one-hot encoding of the result of Argmin operation, only outputting one at leaf node t with $U_{i,t} = 0$; otherwise outputting zero.

For a clearer understanding of our reformulations, a 2-depth tree example is provided in Figure 1. To be correctly assigned to leaf node 5, the sample must pass the branching test at nodes 1 with $\boldsymbol{a}_1^T \boldsymbol{x}_i \leq b_1$ to be directed to left, which implies that $ReLU\left(\boldsymbol{a}_1^T \boldsymbol{x}_i - b_1\right) = 0$. The sample also needs to fail at node 2 to be directed to right with $\boldsymbol{a}_2^T \boldsymbol{x}_i > b_2$, which implies that $ReLU\left(b_2 - \boldsymbol{a}_2^T \boldsymbol{x}_i\right) = 0$. The corresponding violations are $v_{i,1} = 0$ and $v_{i,2} = 0$, leading to a unique zero-violation path with $U_{i,5} = v_{i,1} + v_{i,2}$. For other leaf nodes, the total violations are non-zero (positive). The unique $\mathbb{M}\left(U_{i,5}\right) = 1$ indicates $\boldsymbol{x}_i$ is correctly assigned to leaf 5.

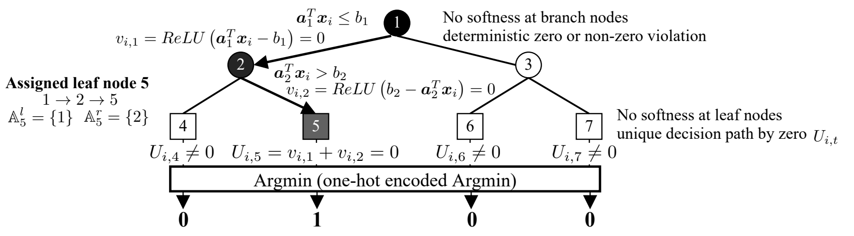

$\boldsymbol{a}_1^T \boldsymbol{x}_i \leq b_1$
1
No softness at branch nodes
deterministic zero or non-zero violation
$v_{i,1} = ReLU\left(\boldsymbol{a}_1^T \boldsymbol{x}_i - b_1\right) = 0$
2
3
$\boldsymbol{a}_2^T \boldsymbol{x}_i > b_2$
$v_{i,2} = ReLU\left(b_2 - \boldsymbol{a}_2^T \boldsymbol{x}_i\right) = 0$
Assigned leaf node 5
$1 \rightarrow 2 \rightarrow 5$
$\mathbb{A}_5^l = \{1\}$ $\mathbb{A}_5^r = \{2\}$
4
5
6
7
No softness at leaf nodes
unique decision path by zero $U_{i,t}$
$U_{i,4} \neq 0$
$U_{i,5} = v_{i,1} + v_{i,2} = 0$
$U_{i,6} \neq 0$
$U_{i,7} \neq 0$
Argmin (one-hot encoded Argmin)
0
1
0
0

Figure 1: Illustrative example for a unique path $1 \rightarrow 2 \rightarrow 5$ of "ReLU+Argmin"-based hard tree.

3.2 Unconstrained optimization for "ReLU+Argmin"-based tree training

Next, we cast reformulated-tree training as an unconstrained optimization task with objective $\mathcal{L}$ as:

$$\mathcal{L} = \sum_{i=1}^{n} \sum_{t \in \mathbb{T}_L} \mathbb{M}\left(U_{i,t}\right) \ell\left(y_i, \hat{y}_i\right). \tag{5}$$

Differentiability analysis of ReLU and Argmin: The trainable variables $\boldsymbol{A}$, $\boldsymbol{b}$, θ are expressed in $v_{i,j}$ and $U_{i,t}$, where ReLU and Argmin are involved. The gradient behavior at ReLU(0) has been extensively studied and is considered theoretically negligible, though numerical effects may arise due to float-point precision [Bertoin et al., 2021]. Consistent with this, we treat it as inconsequential for gradient-based optimization, as evidenced by the success of ReLU networks [Leonardi and Spallanzani, 2020]. Regarding Argmin, to avoid undefined gradient flow at certain points, we use a scaled softmin function to approximate Argmin behaviors in Equation (4).

Scaled softmin to approximate Argmin: Scaled softmin $\mathbb{S}(\cdot)$ is applied to $U_{i,t}$ by Equation (6). Under extreme scaling, softmin ensures that zero-valued $U_{i,t}$ approaches one; otherwise to zero. The scale factor α plays a critical balance between approximation accuracy and optimization stability. Regarding α selection, a larger α yields a closer approximation, but may cause numerical instability, potentially compromising optimization capabilities. Further empirical analyses are given in Appendix B. Identifying optimal α that balances approximation degree and differentiability remains a challenge. To mitigate this, we propose an annealing strategy in Section 4.1 for a better trade-off.

$$\mathbb{S}\left(U_{i,t}\right) = \frac{e^{\alpha(-U_{i,t})}}{\sum_{t \in \mathbb{T}_L} e^{\alpha(-U_{i,t})}}. \tag{6}$$

Notably, this softmin operation is used only during training to facilitate gradient backpropagation. In inference, θ is deterministically recalculated for $\hat{y_i}$, as described in Appendix C. More importantly, it does not introduce softness into sample branching and prediction, as the zero-valued ReLU outputs and violation-free path described in Section 3.1 are established prior to the approximation step.

Following Equation (6), we redefine the optimization task $\mathcal{L}$ in Equation (7).

$$\mathcal{L} = \sum_{i=1}^{n} \sum_{t \in \mathbb{T}_L} \mathbb{S}\left(U_{i,t}\right) \ell\left(y_i, \hat{y_i}\right). \tag{7}$$

4 Differentiable Tree Training via Gradient-based Entire Tree Optimization

Our reformulated task in Equation (7) closely approximates non-differentiable tree training problem, which can be efficiently solved by our proposed entire tree optimization framework.

4.1 Multi-run warm start annealing strategy for scaling softmin operations

Regarding the challenge of selecting an optimal α as earlier discussed for Equation (6), we propose a strategy of multi-run warm start annealing to refine solutions through multiple optimization tasks with increasingly accurate approximations. The annealing has been ever used [Hehn and Hamprecht, 2017, Karthikeyan et al., 2022, Lee and Jaakkola, 2020] to balance the trade-off, though not specifically for our application to softmin. However, their annealing is typically applied within a single training run, such as changing α every few epochs, which may affect stable gradient updates. In contrast, our annealing operates across multiple runs. The solution from an optimization task with a smaller α is used to warm-start the next task with a larger α. By starting with a smaller α and gradually increasing it, this enhances approximation accuracy, while mitigating numerical instability associated with larger α. Detailed steps including sampling of scaled factors $\{\alpha_1, \cdots, \alpha_n\}$ are given in Appendix D, and the implementation is integrated within our tree optimization framework, Appendix G, Algorithm 1. For the α selection, although binary search provides a structured way to explore different α values by evaluating the performance at the midpoint and adjusting α boundaries accordingly, it still involves testing isolated α values without leveraging the solutions from previous α trials. Our subsequent ablation study shows that gradually increasing α, rather than a fixed large value, leads to better training outcomes. We detail binary search comparison in Appendix D.

4.2 Influence of initial values and their adjustments for gradient-based optimization

A good initialization is crucial. Since softmin operates on $U_{i,t}$, which summarizes ReLU-based violations that are either zero or non-zero, samples near decision boundaries ($\boldsymbol{a}_j^T \boldsymbol{x}_i - b_j = 0$) may yield non-zero but near-zero violations. An illustration is given in Appendix E. While such near-zero violations do not affect Argmin behaviors, which only select the unique path with $U_{i,t} = 0$, they can sensitively affect softmin. Specifically, softmin may fail to ideally produce a value close to one, reducing approximation accuracy. A bad initial solution for $\boldsymbol{A}$ and $\boldsymbol{b}$ can result in a poor optimization outcome. To mitigate this, $\boldsymbol{A}$ and $\boldsymbol{b}$ can be adjusted to maximize the margin between the decision boundary and nearest samples, without altering existing sample assignments as illustrated by green line in Appendix E, Figure 3. This adjustment can be easily achieved either by calculating the median of $\boldsymbol{a}_j^T \boldsymbol{x}_i$ for the closest samples on both sides of the boundary, or using support vector machine to treat sample assignments as a binary classification task with explanations in Appendix E.

Noticeably, this strategy mainly handles cases where $\boldsymbol{a}_j^T \boldsymbol{x}_i - b_j \approx 0$. However, it becomes ineffective in the corner case where $\boldsymbol{a}_j = 0$ and $b_j = 0$ with same violations for all leaves. This limitation can impair optimization. To mitigate this, we typically incorporate this strategy with multiple random initializations. Fortunately, our extensive experiments show that such corner cases appear to be extremely rare in practice, and we have not observed noticeable performance degradation.

4.3 Differentiable decision tree optimization framework

Unlike greedy methods that optimize each node sequentially, our approach concurrently optimizes the entire tree, including $\boldsymbol{A}$ and $\boldsymbol{b}$ at all branch nodes and θ at all leaf nodes. Our "**R**eLU+**A**rgmin"-based **D**ifferentiable **D**ecision **T**ree (termed `RADDT`), outlined in Appendix G, Algorithm 1, begins at multiple random initialization (*Line 4 - 5*). This increases the chance of finding better solutions. Each initialization is adjusted to achieve the maximum margin (*Line 4*). For each start, the optimization with our annealing is conducted to produce a tree candidate (*Line 6 - 15*). The final optimal tree is selected by comparing candidates from multiple starts, with each evaluated using deterministic leaf predictions and exact loss calculations without approximation (*Line 11 - 13*). This framework is readily implementable using existing tools like PyTorch. Despite the introduction of additional hyperparameters in gradient-based optimization, tuning them is not typically necessary because their effects are straightforward. More empirical analyses are detailed in Appendix F.

5 Numerical Experiments and Discussions

We mainly evaluate regression tasks, but also include the same classification datasets used by certain baselines for a more convincing comparison. Our tree with constant or linear predictions, termed the respective `RADDT` and `RADDT-Linear`, is compared against a broad range of trees in testing accuracy, training optimality and training time. The **14 baselines** include: **(a)** greedy `CART`, `HHCART`, `RandCART`, and `OC1`; **(b)** non-greedy `TAO` [Zharmagambetov and Carreira-Perpinan, 2020]; **(c)** gradient-based trees using STE like `GradTree` [Marton et al., 2023], `DGT` [Karthikeyan et al., 2022] and `DTSemNet` [Panda et al., 2024]; **(d)** sigmoid-based soft tree `SoftDT` [Frosst and Hinton, 2017]; **(e)** relaxed MIP-based tree solved via implicit differentiation `LatentTree` [Zantedeschi et al., 2021]; **(f)** local search `ORT-LS` [Dunn, 2018]; **(g)** soft tree variant using smooth-step function `TEL` [Hazimeh et al., 2020] (Tree ensemble); **(h)** other ensembles like random forest `RF` and `XGBoost`. Our primary focus is on comparing oblique trees. The inclusion of orthogonal `CART` serves as a foundational work, aligning with prior work on oblique trees, such as `TAO`, `DGT`, `DTSemNet` and `TEL`, which also use `CART` for comparison. Although outperforming `CART` is an expected outcome, its inclusion helps quantify the amount of improvements achievable by oblique tree. `GradTree` is included to enable a fair comparison against other STE-based oblique trees like `DGT` and `DTSemNet`. Since it remains uncertain whether oblique trees can match tree ensemble's accuracy, we include `RF` and `XGBoost` as a commonly used and strong ensemble baselines, and `TEL` as the oblique ensemble counterpart.

These 14 baseline comparisons are conducted across **four groups of datasets**: **(i)** 17 medium-sized regression datasets with fewer than 41k samples (primary focus); **(ii)** 27 classification and 9 regression datasets used in the papers of certain baselines (for a more credible comparison); **(iii)** 4 real-world datasets with about 100 samples, and 3 synthetic datasets with 5000 samples (for comparing global optimality with global tree `ORT-MIP` [Bertsimas and Dunn, 2017] and known ground truth); **(iv)** 7 large-scale datasets each with at least 1 million samples (for evaluating scalability).

Detailed dataset information and usage are given in Appendix H. Comparisons focus on accuracy in Coefficient of Determination (usually denoted as R^2), and computational time in seconds. The Friedman Rank [Sheskin, 2020] is also used to statistically sort the compared methods according to their testing accuracy, with a lower value indicating better performance. Comprehensive details on the implementation for each compared method, and computing facilities are given in Appendix I.

5.1 Testing accuracy comparison

To evaluate the testing accuracy of our optimized tree, we compare it against diverse decision trees and 3 tree ensembles with different tree induction methods. For a fair comparison, we conduct depth tuning for all tree methods to select the optimal tree depth from 1 to 12 (except for `CART` from 1 to 100 due to its tendency to rely on deeper depth for higher accuracy).

Comparison against other decision trees: In Table 1, our `RADDT` consistently outperforms compared trees in test accuracy across Group (i) 17 datasets. Specifically, `RADDT` surpasses the foundational `CART` by 7.54%, greedy `HHCART` by 5.64%, and `ORT-LS` by 3.72%. These results underscore the effectiveness of our tree optimization. Besides, Friedman rank comparisons reinforce these findings, with `RADDT` attaining the highest rank. Detailed results for each dataset are provided in Appendix K.1.

Regarding existing gradient-based trees, since `DGT` and `LatentTree` fail to scale to depth 12, we evaluate them under another fixed-depth setting in Section 5.2. `GradTree`, as observed in Table 1, performs poorly in our experiments. This result is within our expectations, as their original paper reports that `GradTree` underperforms `CART` on 17 out of 36 datasets (see their Table 1 and 2 in [Marton et al., 2023]). Nonetheless, to ensure a more credible comparison, we further evaluate our

Table 1: Test accuracy for compared decision trees on 17 medium-sized datasets in Group (i).

	Greedy Methods				Gradient-based[1, 2]		Local Search	Ours
	`CART`	`RandCART`	`HHCART`	`OC1`	`GradTree`	`SoftDT`	`ORT-LS`	`RADDT`
Testing Accuracy (R^2, %)	74.85	71.20	76.75	73.31	64.30	72.72	78.67	**82.39**
Tree Depth	10.24	8.12	8.29	8.12	10.29	10.29	6.24	7.29
Friedman Rank	4.65	5.88	3.65	5.06	7.00	4.76	3.24	**1.76**

[1] Other two gradient-based `DGT` and `LatentTree` are compared in Table 3 with fixed depths due to scalability issues at depth 12.
[2] More credible results on their originally-used dataset are discussed below, include `GradTree`, `SoftDT`, `DGT`, and `DTSemNet`.

method on the same classification datasets used in their study. Similar same-dataset comparisons are also conducted for `SoftDT`, `DGT-Linear`, `DTSemNet` and non-greedy `TAO-Linear` as below.

A more credible same-dataset comparison on Group (ii) datasets originally used by five baselines: For a more convincing comparison, we evaluate on the same datasets used in the original works of five baselines: 27 classification datasets in `GradTree`, 4 regression datasets in soft tree [İrsoy et al., 2012], and 5 shared regression datasets among `DGT-Linear`, `TAO-Linear` and `DTSemNet`. Dataset information is given in Appendix H. Besides using same datasets, we also compare directly with the results reported in their own papers. For fairness, our method is evaluated using each baseline's experimental setup, including same data preprocessing and evaluation metrics. Full implementation details are given in Appendix K.2. For `GradTree`, with detailed results for each dataset given in Appendix K.3, Table 15, our method outperforms `GradTree`'s reported testing results by an average of 4.99%. Regarding soft tree, results in Appendix K.4, Table 16, show that `RADDT` achieves 6.88% higher test accuracy, again aligning with prior trends. Regarding `DGT-Linear`, `TAO-Linear` and `DTSemNet`, the `DTSemNet` work directly reports `TAO-Linear`'s original results due to the absence of open-source code for `TAO-Linear`. Since `DTSemNet` itself is a tree with linear predictions, for consistency, it adapts the original `DGT` tree with constant predictions to a linear variant `DGT-Linear`. Following this comparison from `DTSemNet`, we extend `DTSemNet`'s Table 4 by including our results under same experimental setup. As in Appendix K.5, Table 17, ours outperforms these baselines on 4 out of 5 datasets (except "YearPred"), achieving the best average rank of 1.6, followed by `DTSemNet` with 2.4, `TAO-Linear` with 2.6, and `DGT-Linear` with 3.2, further supporting our previous findings.

Statistical analysis regarding Table 1: While Table 1 empirically shows that `RADDT` is superior to the other compared trees, we further conduct a paired T-test to statistically validate the significant difference among these tree methods. The null hypothesis asserts that `RADDT` is not significantly different from other trees. If calculated p-value is less than tolerance τ, the null hypothesis can be rejected, indicating statistical significance. The t-statistic (black point), p-value and 95% confidence are shown in Figure 2. The results for all comparisons with $p < \tau = 0.1$ and positive t-statistics consistently indicate that `RADDT` is superior to these compared decision trees with statistical significance.

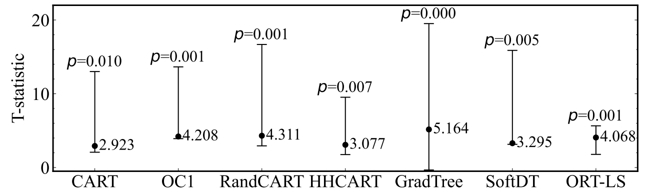

Figure 2: Paired T-test comparing `RADDT` with other trees (setting significance level $\tau = 0.1$).

Comparison against tree ensembles on Group (i) 17 datasets: Following decision tree comparison, we proceed to compare our method with `RF`, `XGBoost` and `TEL` to validate its competitive accuracy. Our `RADDT` slightly underperforms tree ensembles on average. In contrast, `RADDT-Linear` outperforms `RF` by 2.01%, `XGBoost` by 1.12% and `TEL` by 0.76%, as shown in Table 2. The superiority of `RADDT-Linear` is further supported by Friedman rank, where `RADDT-Linear` ranks highest, matching that of `XGBoost`. Detailed results for each dataset are provided in Appendix K.1. These findings highlight that our method even performs competitively compared to tree ensembles. For a fair comparison with tree ensembles, this experiment has performed a hyperparameter tuning with 300-combination search, including depth up to 50 and number of trees up to 500, following guidelines from [Oshiro et al., 2012, Probst et al., 2019]. Detailed tuning procedures are given in Appendix J. In addition to this 300-combination parameter tuning for ensembles, we also conduct a more extensive tuning like 10,000-combination search in Appendix K.6. Despite extensive tuning, our key findings remain unchanged, and the statistical Friedman rank shows no significant difference. Importantly, our aim is not to claim superiority over ensembles. Since any base learner can be improved via ensembling like bagging, comparing a single tree to ensembles is inherently unfair. Instead, we provide a reference showing that our tree can match ensemble's accuracy with far fewer parameters.

Table 2: Test accuracy for our trees and 3 tree ensembles on 17 medium-sized datasets in Group (i).

	`RF`	`XGBoost`	`TEL`	`RADDT`	`RADDT-Linear`
Number of Trees	314.71	352.94	10	1	1
Test Accuracy (R^2, %)	82.62	83.51	83.87	82.39	**84.63**
Friedman Rank	2.88	**2.24**	3.29	4.35	**2.24**

5.2 Superior testing accuracy analysis: from training optimality perspective

To figure out the reason behind the superior testing accuracy, we then analyze the optimality of training. Training trees with different depths correspond to different optimization tasks. To assess optimality, training trees at fixed depth is a common practice. Fixed depths of $D = \{2, 4, 8, 12\}$ are used for comparison. Table 3 shows that our `RADDT` outperforms `ORT-LS` by 5.35%, 2.66% and 0.02% in training accuracy for depths of 2, 4, and 8, respectively, while it outperforms `CART` by 24.83%, 21.02% and 9.48% across various depths. For other gradient-based trees, `RADDT` significantly outperforms `GradTree` and `SoftDT` on average at all depths. `LatentTree` and `DGT` do not scale to depth 12. On average across these feasible depths, our method outperforms `LatentTree` by 10.39% in training and 6.24% in testing accuracy, and surpasses `DGT` by 7.52% in training and 2.66% in testing accuracy. Improvements in training accuracy imply that our optimization algorithm achieves better training optimality. Furthermore, an increase in training accuracy correlates with the improved test accuracy at depths of 2, 4, and 8, suggesting that an optimized tree with higher training accuracy can potentially yield better test accuracy before encountering serious overfitting issues. Overfitting, particularly at a depth of 12, is simply addressed by tuning an optimal tree depth. The overfitting limitation is further analyzed in Section 5.6.

Table 3: Fixed-depth comparison of training, testing accuracy and training time on Group (i) datasets.

	D	Greedy Methods				Gradient-based Trees				Local Search	Ours
		`CART`	`RankCART`	`HHCART`	`OC1`	`GradTree`	`SoftDT`	`DGT`	`LatenTree`	`ORT-LS`	`RADDT`
Train (R^2,%)	2	46.95	32.81	46.20	49.59	39.42	50.59	64.48	66.94	66.43	**71.78**
	4	61.16	54.09	62.65	63.21	53.29	56.83	75.83	72.25	79.52	**82.18**
	8	81.45	77.51	82.26	81.43	64.65	66.81	82.01	74.54	90.91	**90.93**
	12	93.45	93.06	94.74	93.02	66.86	73.03	/	/	97.46	96.36
Test (R^2,%)	2	46.14	32.47	45.61	47.95	38.53	49.94	63.81	66.42	64.51	**70.07**
	4	58.92	52.69	61.30	60.22	51.45	56.32	75.16	71.03	75.06	**78.98**
	8	69.77	69.93	74.57	69.08	62.40	66.44	79.99	70.77	74.93	**77.89**
	12	68.28	64.13	68.37	65.57	63.81	72.45	/	/	68.25	**73.11**
Time (s)	2	0.03	0.70	4.43	3,216	31.32	22.24	2,102	1,624	457.21	542.22
	4	0.04	1.56	7.45	4,192	54.74	81.88	2,577	2,194	868.08	478.81
	8	0.07	5.08	12.52	4,803	298.92	1,209	4,049	2,381	9,336	602.69
	12	0.10	12.61	22.01	5,103	10,417	54,829	/	/	210,141	2,643

Training optimality comparison against global optimal solutions on Group (iii) datasets: The above results reveal that our approach achieves superior training optimality. To provide a reference for global optimality, we then compare it with global optimal trees `ORT-MIP`. However, `ORT-MIP` fails to find optimal trees for any of the above datasets, even with 128 cores and a two-day time limit. It can only solve a 2-depth tree on 4 small datasets in Group (iii) to a global optimum with 1% optimality gap. Despite the existence of sparse optimal trees [Zhang et al., 2023], a direct comparison is infeasible for some reasons discussed in Appendix K.7. We also detail train accuracy comparison there. Results show that `RADDT` nearly reaches global optimum (`ORT-MIP`) with 2.82% discrepancy.

Training optimality comparison against ground truth on Group (iii) datasets: We further evaluate `RADDT` on three synthetic datasets with known ground truth, each with 5000 samples. The procedure for generating synthetic datasets is detailed in Appendix H. The corresponding ground truths for training and testing accuracy are 100%. In Appendix K.8, Table 20, our `RADDT` closely approximates global optimality in training and testing accuracy, with 0.64% difference over ground truth on average. These results, together with the previous global solution comparisons, further validate the effectiveness of our tree optimization.

Ablation study on the optimization strategies: The notable training accuracy of our `RADDT` method can be attributed to two key strategies designed to enhance approximation accuracy: the multi-run warm start annealing strategy, which improves training accuracy by an average of 7.1% across various depths compared to standard softmin function without any scaling; and the strategy of adjusting initial solutions for gradient-based optimization, which contributes an additional 1.8% improvement on average. Detailed results for the ablation study are provided in Appendix K.9.

5.3 Scalability assessment to 12-depth trees on 7 million-scale datasets in Group (iv)

Previous experiments focus on three different groups of datasets with fewer than 41k samples. To further evaluate our scalability, we test it on seven large-scale datasets, each containing at least 1 million samples, using the same fixed-depth setting as in Table 3. The Group (iv) dataset is detailed in Appendix H. As shown in Appendix K.10, Table 22, our `RADDT` successfully scales to a 12-depth tree, outperforming `CART` by 4.83% in training and 3.15% in testing across all depths. In contrast, `GradTree` and `SoftDT` fail to output good solutions. At the feasible depths for `DGT` and `LatentTree`, `RADDT` outperforms `DGT` by 3.9% in training and 3.74% in testing on average, while it slightly underperforms `LatentTree` by 0.03% in training and 0.08% in testing. However, `RADDT` takes significantly less training time, and `LatentTree` is only solvable at depths 2 and 4. These comparisons effectively showcase `RADDT`'s scalability on million-scale datasets at depth-12 trees.

GPU acceleration and training time analysis: Our training time is primarily affected by sample size n, feature number p and depth D. For D-depth tree training, each sample must be evaluated at all $2^D - 1$ branch nodes via matrix operation $\boldsymbol{A}\boldsymbol{x}_i$, requiring $\mathcal{O}(p \cdot (2^D - 1))$ operations per sample and $\mathcal{O}(n \cdot p \cdot (2^D - 1))$ operations for the full dataset. It indicates that training time increases with larger n and D. Importantly, our implementation is highly parallelizable and facilitates multi-GPU acceleration. The specific GPU configurations in our experiments and acceleration analysis are given in Appendix K.11. In the million-scale comparison Appendix K.10, Table 22, our `RADDT` achieves a 42-fold speedup over `DGT` at depth 4. These scalability advantages become even more pronounced with deeper trees and more samples, where larger matrix operations dominate the computation. However, in this setting within Table 22, most high-accuracy baselines fail to scale to depth 12, making direct comparisons at that depth infeasible. To further illustrate the advantage, we refer to Table 3, where the second-best method `ORT-LS` scales to depth 12. For instance, on the "ailerons" dataset, `RADDT` is 432 times faster than `ORT-LS`, demonstrating the substantial speedup at deeper depths. Detailed time comparisons for datasets with more than 10,000 samples used in Table 3 are given in Appendix K.12. Besides, a training time comparison of our method in GPU versus CPU settings is provided in Appendix K.13, although the advantages of GPU acceleration are expected.

5.4 Analysis of model complexity and inference time

Alongside tree depth, the number of model parameters also offers a clear view of model complexity. While oblique tree typically requires more parameters than orthogonal tree at a given depth due to feature combinations, it often yields better accuracy with much smaller depth. Therefore, for a similar accuracy, our oblique tree may not require more parameters overall than orthogonal tree.

For a D-depth binary tree with $\mathbb{T}_B = 2^D - 1$ branch nodes and $\mathbb{T}_L = 2^D$ leaf nodes, and a dataset with p features, orthogonal tree like CART requires $2 \cdot \mathbb{T}_B + \mathbb{T}_L$ parameters. In contrast, our oblique tree `RADDT` requires $\mathbb{T}_B \cdot p + 1 + \mathbb{T}_L$ parameters, while our `RADDT-Linear` needs $\mathbb{T}_B \cdot p + 1 + \mathbb{T}_L \cdot p + 1$ parameters. Based on these, we compare the number of model parameters for `CART`, `RADDT` and `RADDT-Linear` in Table 4 by averaging across all Group (i) 17 datasets. As shown in Table 4, `CART` achieves 74.85% accuracy with average depth 10.24 and 3,140.94 parameters. Our `RADDT` and `RADDT-Linear` reach 82.39% and 84.63% accuracy at depths 7.29 and 4.82, using 10,503.94 and 4,044.71 parameters, respectively. Notably, if the goal is to match or slightly exceed `CART`'s accuracy, our models can do so with much smaller trees. Table 4 shows that `RADDT` achieves 75.23% at depth 2.82 using only 101.71 parameters, and `RADDT-Linear` reaches 77.21% at depth 1 with just 40.47 parameters, yielding 31 times and 78 times reductions in parameter count compared to `CART`. These results indicate that our methods do not necessarily require more parameters for improved accuracy; the total parameter cost depends on the desired trade-off between accuracy and model complexity.

Additionally, inference time greatly helps assess model complexity. In the setting of Table 1 and Table 2, our methods achieves superior accuracy improvements but involves more parameters than `CART`, resulting in slightly higher inference time. However, if only aiming to achieve an accuracy comparable to `CART` (74.85%), Table 4 shows that the inference time of `RADDT` becomes comparable to `CART`, while `RADDT-Linear` is even faster. It is important to note that our implements use Python

Table 4: Model complexity and inference time comparison with CART on Group (i) 17 datasets.

Method	Testing Accuracy (R^2, %)	Depth	Number of Branch Nodes	Number of Leaf Nodes	Total Number of Model Parameters	Inference Time (Millisecond)
CART	74.85 (reported in Table 1)	10.24	1,046.65	1,047.65	3,140.94	0.44
RADDT	82.39 (reported in Table 3)	7.29	671.94	672.94	10,503.94	1.88
	75.23 (only slightly exceed CART's accuracy)	2.82	6.88	7.88	101.71	0.54
RADDT-Linear	84.63 (reported in Table 3)	4.82	129	130	4,044.71	1.61
	77.21 (only slightly exceed CART's accuracy)	1	1	2	40.47	0.39

and PyTorch, where inference time may not scale strictly with parameter count due to framework overhead. A pure C++ implementation would likely align more closely with parameter count.

5.5 Interpretability analysis

We fully acknowledge that orthogonal trees like CART, at the same depth, are generally more interpretable than oblique trees. However, as originally analyzed in OC1 [Murthy et al., 1994], oblique trees could become more interpretable when their depth is substantially smaller. Interpretability depends on multiple factors including tree depth, feature number, and the accuracy-simplicity trade-off. There is no interpretability superiority of one approach over the other, as it depends on specific application scenarios. We evaluate our RADDT's interpretability from three aspects: tree-based prediction logic, unique prediction path and the complexity of decision rules. Detailed analysis can be found in Appendix K.14 with an illustrative example in Figure 7.

5.6 Limitations analysis and future work

While our approach achieves superior accuracy, several limitations remain. The primary limitation lies in inadequate regularization. In Table 3, while training accuracy for RADDT improves by 5.43% from depth 8 to 12, testing accuracy conversely drops by 4.78%, indicating a serious overfitting issue. This issue is more pronounced in trees with linear predictions, as detailed in Appendix K.15. In response, we apply preliminary $L1$ regularization to RADDT-Linear for experiments in Table 2, leading to a modest 0.57% improvement in testing accuracy. Due to the challenges in identifying optimal regularization strength and potential increases in training time, we just used a small value of $1e-4$, without extensive tuning. Despite this, further improvements could be achieved through more dedicated regularization strategies, such as the post-hoc regularization technique, Hierarchical Shrinkage, proposed for trees by Agarwal et al. [2022]. Second, the effectiveness of our multi-run warm start annealing strategy is validated by empirical observations; however, a theoretical analysis is still lacking. Third, our tailored initialization adjustment strategy fails to consider the corner case of an ill-defined initialization where both $\boldsymbol{a}_j = 0$ and $b_j = 0$. This is also a limitation, despite its rarity and minimal impact on empirical performance in practice. Fourth, while our current hyperparameter tuning for tree ensembles is sufficient to support our main claims, especially given that our goal is not to claim superiority over ensembles, more tuning on regularization parameters could potentially yield even better results for tree ensembles. Exploring this gap between a single tree and ensembles presents a promising area for future research. Next interesting future direction is to apply our optimization strategies, such as initialization and multi-run warm-start annealing, to other gradient-based trees like SoftDT. Since these strategies are general, they are not limited to our specific tree formulation and may benefit other models. Another promising alternative to our scaled softmin approximation is the Entmax function. However, its application requires further investigation, as selecting its sparsity parameter presents a similar challenge to choosing the scale factor in our softmin method.

6 Conclusion

Our approach addresses two main limitations of classic decision tree: non-differentiability and low test accuracy, thereby enhancing its practicality. We tackle these issues by first proposing a "ReLU+Argmin"-based hard split tree with a novel exact reformulation, then significantly improving its test accuracy through our gradient-based entire tree optimization. The entire tree training problem is reformulated as an unconstrained optimization task, with a scaled softmin function approximating Argmin behaviors for effective gradient backpropagation. Our reformulated tree, unlike existing soft approximation, eliminates the softness at both branch nodes and leaf nodes, thus preserving hard splits and deterministic predictions. Extensive experiments demonstrate our tree's superior accuracy and scalability on million-scale datasets.

Acknowledgments and Disclosure of Funding

Yankai Cao acknowledges funding from discovery program of the Natural Science and Engineering Research Council of Canada (RGPIN-2019-05499) and New Frontiers in Research Fund (NFRFE-2022-00663). The authors also gratefully acknowledge the computing resources and services provided by Digital Research Alliance of Canada (www.alliancecan.ca), and Advanced Research Computing at the University of British Columbia.

References

Daniël Vos and Sicco Verwer. Optimizing interpretable decision tree policies for reinforcement learning, 2024. URL `http://arxiv.org/abs/2408.11632`.

Sascha Marton, Tim Grams, Florian Vogt, Stefan Lüdtke, Christian Bartelt, and Heiner Stuckenschmidt. Mitigating information loss in tree-based reinforcement learning via direct optimization, 2025. URL `http://arxiv.org/abs/2408.08761`.

Vinícius G. Costa and Carlos E. Pedreira. Recent advances in decision trees: An updated survey. *Artificial Intelligence Review*, 56(5):4765–4800, 2023. doi: 10.1007/s10462-022-10275-5.

Haoran Zhu, Pavankumar Murali, Dzung Phan, Lam Nguyen, and Jayant Kalagnanam. A scalable mip-based method for learning optimal multivariate decision trees. In *Advances in Neural Information Processing Systems*, volume 33, pages 1771–1781. Curran Associates, Inc., 2020.

Leo Breiman, Jerome Friedman, Charles J. Stone, and R. A. Olshen. *Classification and Regression Trees*. Taylor & Francis, 1984. ISBN 978-0-412-04841-8.

S. K. Murthy, S. Kasif, and S. Salzberg. A system for induction of oblique decision trees. *Journal of Artificial Intelligence Research*, 2:1–32, 1994. doi: 10.1613/jair.63.

D. C. Wickramarachchi, B. L. Robertson, M. Reale, C. J. Price, and J. Brown. Hhcart: An oblique decision tree, 2015.

Rico Blaser and Piotr Fryzlewicz. Random rotation ensembles. *Journal of Machine Learning Research*, 17(4):1–26, 2016.

Arman Zharmagambetov and Miguel Carreira-Perpinan. Smaller, more accurate regression forests using tree alternating optimization. In *Proceedings of the 37th International Conference on Machine Learning*, pages 11398–11408. PMLR, 2020.

Dimitris Bertsimas and Jack Dunn. Optimal classification trees. *Machine Learning*, 106(7):1039–1082, 2017. doi: 10.1007/s10994-017-5633-9.

Jimmy Lin, Chudi Zhong, Diane Hu, Cynthia Rudin, and Margo Seltzer. Generalized and scalable optimal sparse decision trees, 2022. URL `http://arxiv.org/abs/2006.08690`.

Justin Boutilier, Carla Michini, and Zachary Zhou. Optimal multivariate decision trees. *Constraints*, 2023. doi: 10.1007/s10601-023-09367-y.

Jack William Dunn. *Optimal Trees for Prediction and Prescription*. Thesis, Massachusetts Institute of Technology, 2018.

Ajaykrishna Karthikeyan, Naman Jain, Nagarajan Natarajan, and Prateek Jain. Learning accurate decision trees with bandit feedback via quantized gradient descent, 2022.

Sascha Marton, Stefan Lüdtke, Christian Bartelt, and Heiner Stuckenschmidt. Learning decision trees with gradient descent, 2023.

Subrat Prasad Panda, Blaise Genest, Arvind Easwaran, and Ponnuthurai Nagaratnam Suganthan. Vanilla gradient descent for oblique decision trees, 2024.

Ozan İrsoy, Olcay Taner Yıldız, and Ethem Alpaydın. Soft decision trees. In *Proceedings of the 21st International Conference on Pattern Recognition (ICPR2012)*, pages 1819–1822, 2012.

Alvin Wan, Lisa Dunlap, Daniel Ho, Jihan Yin, Scott Lee, Henry Jin, Suzanne Petryk, Sarah Adel Bargal, and Joseph E. Gonzalez. Nbdt: Neural-backed decision trees, 2021.

Nicholas Frosst and Geoffrey Hinton. Distilling a neural network into a soft decision tree, 2017.

Hussein Hazimeh, Natalia Ponomareva, Petros Mol, Zhenyu Tan, and Rahul Mazumder. The tree ensemble layer: Differentiability meets conditional computation. In *Proceedings of the 37th International Conference on Machine Learning*, pages 4138–4148. PMLR, 2020.

Yongxin Yang, Irene Garcia Morillo, and Timothy M. Hospedales. Deep neural decision trees, 2018.

Mohammad Norouzi, Maxwell Collins, Matthew A Johnson, David J Fleet, and Pushmeet Kohli. Efficient non-greedy optimization of decision trees. In *Advances in Neural Information Processing Systems*, volume 28. Curran Associates, Inc., 2015. URL `https://proceedings.neurips.cc/paper/2015/hash/1579779b98ce9edb98dd85606f2c119d-Abstract.html`.

Guang-He Lee and Tommi S. Jaakkola. Oblique decision trees from derivatives of relu networks, 2020. URL `http://arxiv.org/abs/1909.13488`.

Stephen Gould, Basura Fernando, Anoop Cherian, Peter Anderson, Rodrigo Santa Cruz, and Edison Guo. On differentiating parameterized argmin and argmax problems with application to bi-level optimization, 2016.

Valentina Zantedeschi, Matt Kusner, and Vlad Niculae. Learning binary decision trees by argmin differentiation. In *Proceedings of the 38th International Conference on Machine Learning*, pages 12298–12309. PMLR, 2021.

Qiangqiang Mao and Yankai Cao. Can a single tree outperform an entire forest?, 2024. URL `http://arxiv.org/abs/2411.17003`.

J. R. Quinlan. Learning with continuous classes. In *Proceedings Australian Joint Conference on Artificial Intelligence.*, pages 343–348, Singapore, 1998. World Scientific. URL `http://www.researchgate.net/publication/2627892_Learning_With`.

David Bertoin, Jérôme Bolte, Sébastien Gerchinovitz, and Edouard Pauwels. Numerical influence of relu'(0) on backpropagation. In *Advances in Neural Information Processing Systems*, volume 34, pages 468–479. Curran Associates, Inc., 2021.

Gian Paolo Leonardi and Matteo Spallanzani. Analytical aspects of non-differentiable neural networks, 2020.

Thomas Hehn and Fred A. Hamprecht. End-to-end learning of deterministic decision trees, 2017.

David J. Sheskin. *Handbook of Parametric and Nonparametric Statistical Procedures, Fifth Edition*. CRC Press, 2020. ISBN 978-1-4398-5804-2.

Thais Mayumi Oshiro, Pedro Santoro Perez, and José Augusto Baranauskas. How many trees in a random forest? In *Machine Learning and Data Mining in Pattern Recognition*, pages 154–168, Berlin, Heidelberg, 2012. Springer. ISBN 978-3-642-31537-4. doi: 10.1007/978-3-642-31537-4_13.

Philipp Probst, Marvin N. Wright, and Anne-Laure Boulesteix. Hyperparameters and tuning strategies for random forest. *WIREs Data Mining and Knowledge Discovery*, 9(3):e1301, 2019. doi: 10.1002/widm.1301. URL `https://onlinelibrary.wiley.com/doi/abs/10.1002/widm.1301`.

Rui Zhang, Rui Xin, Margo Seltzer, and Cynthia Rudin. Optimal sparse regression trees. *Proceedings of the AAAI Conference on Artificial Intelligence*, 37(9):11270–11279, 2023. doi: 10.1609/aaai.v37i9.26334. URL `https://ojs.aaai.org/index.php/AAAI/article/view/26334`.

Abhineet Agarwal, Yan Shuo Tan, Omer Ronen, Chandan Singh, and Bin Yu. Hierarchical shrinkage: Improving the accuracy and interpretability of tree-based models. In *Proceedings of the 39th International Conference on Machine Learning*, pages 111–135. PMLR, 2022. URL `https://proceedings.mlr.press/v162/agarwal22b.html`.

Dheeru Dua and C. Graff. UCI machine learning repository., 2019.

Joaquin Vanschoren, Jan N. van Rijn, Bernd Bischl, and Luis Torgo. Openml: Networked science in machine learning. *SIGKDD Explor. Newsl.*, 15(2):49–60, 2014. doi: 10.1145/2641190.2641198. URL `https://dl.acm.org/doi/10.1145/2641190.2641198`.

Appendices for:
Differentiable Decision Tree via "ReLU+Argmin" Reformulation

A Certain Scenarios Requiring Decision Trees with Hard-splits

Hard-split decision trees and soft decision trees represent fundamentally different models, each suited to different application scenarios. Further, there do exist scenarios where the application of hard-split decision trees is not only more appropriate but also imperative. Below is an illustrative example from industrial projects that underscores this preference.

Scenario: Piece-wise affine control law in explicit model predictive control.

In explicit model predictive control, the control law is often represented by piece-wise affine functions, which can be effectively approximated by a hard-split decision tree. The hard decisions at branch nodes can be used to determine the control action based on the state of the system, which can be easily implemented in real-time control systems.

Beyond the utility of making clear hard decisions, the optimal decision tree model that offers superior predictive performance is also crucial for these scenarios. From the perspective of application scenarios, the motivation and necessity for hard-split optimal decision trees are intuitive and compelling.

B Empirical Analysis of Scale Factor Impacts on Scaled Softmin Operation

The scale factor α significantly influences the approximation degree to Argmin function and the behavior of its gradient in optimization. A larger α leads to a better approximation than standard softmin function with $\alpha = 1$, achieving closer proximity to an Argmin function as α approaches infinity. An illustration for the gap between scaled softmin function and the Argmin function under varying α is shown in Figure 6. Nonetheless, a larger α also results in a more unstable gradient, which may adversely affect the optimization process. Consequently, the α represents a critical balance between achieving high approximation degree and maintaining stability in optimization processes.

To show how the scale factor α impacts the training optimality of the unconstrained optimization problem (our `RADDT` method without using the strategy of multi-run warm start annealing), we conduct comparison experiments across different α values at different depths. Our differentiable decision tree optimization framework will be introduced in Section 4. The findings, summarized in Table 5, reveal the relationship between α and training performance, as measured by the average training accuracy R^2. Notably, we observe that the training accuracy at the extremes of $\alpha = 1$ (standard softmin function) and $\alpha = 1000$ are inferior compared to intermediate α values. This observation underscores two critical insights: first, relying solely on softmin function ($\alpha = 1$) yields suboptimal optimization results; second, the high α value may not necessarily lead to better optimality.

Table 5: The impact of α on training accuracy across different depths.

Various α Value	Training Accuracy (%)			
	$D = 2$	$D = 4$	$D = 8$	$D = 12$
$\alpha = 1$ (Standard Softmin Function)	60.78	69.97	81.46	93.45
$\alpha = 20$	70.28	79.43	87.98	94.49
$\alpha = 150$	68.00	78.31	88.08	94.42
$\alpha = 1000$	65.05	74.16	83.79	93.45

However, it remains a challenge to identify the optimal scale factor α that balances the trade-off between approximation degree and differentiability. To mitigate this issue, we propose a multi-run warm start annealing strategy, detailed in the following Section 4.1, to narrow the gap between the Argmin behaviors and its differentiable approximation.

C Deterministic Calculations for Leaf Prediction Parameters

As detailed in Section 3.2, our method deterministically calculates the leaf prediction parameters θ (i.e., the parameters $\boldsymbol{K}$ and $\boldsymbol{h}$ in regression, and the parameters $\boldsymbol{h}$ in classification), instead of directly using trained values for θ. Given a tree with tree split parameters $\boldsymbol{A}$ and $\boldsymbol{b}$, the deterministic tree path for each sample can be obtained, which allows determining the total number of samples assigned to a specific leaf node $t \in \mathbb{T}_L$.

In classification tasks, the value of $\boldsymbol{h}$ at a leaf node t corresponds to the majority class among the samples assigned to that leaf node. In this case, the leaf value is represented as a class label or the one-hot vector specific to the class, $h_t \in \{0, 1\}^c$, in contrast to the continuous value $h_t \in R^c$ used during the training phase.

In regression tasks, we consider two types of leaf prediction: linear prediction and constant prediction. For decision trees with linear predictions, the prediction at a leaf node is a linear combination of input features by fitting a linear correlation between all samples assigned to that leaf node. The leaf values at a leaf node t, $\boldsymbol{k}_t$ and h_t, are the linear coefficients determined by linear regression. For decision trees with constant predictions, the value of $\boldsymbol{K}$ remains zero. The value of $\boldsymbol{h}$ at a leaf node t is an average of the true output values (y_i) of the samples assigned to that leaf node t.

D Implementation Details of Multi-run Warm Start Annealing

As discussed in Section 4.1, the key challenge in enhancing the approximation accuracy to Argmin behaviors lies in the selection of α. A larger α may destabilize optimization process, whereas a smaller α tends to be easier to solve for gradient-based optimization. The annealing strategy, which gradually changes α from small to large values, has been ever used to strike such a balance in existing literature [Hehn and Hamprecht, 2017, Karthikeyan et al., 2022, Lee and Jaakkola, 2020], though not specifically for our application to scaled softmin. However, their annealing typically adjusts α within a single training process, such as changing α every few epochs, which may affect stable gradient updates. Besides, the implementation details in these works are not well-documented. Considering these, we introduce a detailed description of our annealing strategy.

Our annealing process operates across multiple optimization runs with different α values. The solution from an optimization task with a smaller α is used to effectively warm-start the next optimization run with a larger α. By starting with a smaller scale factor and gradually increasing it, this strategy enhances the approximation accuracy, while mitigating numerical instability typically associated with larger scale factors.

Specifically, the procedure begins by sampling a set of scale factors within a predetermined range from the smallest α_{min} to the largest α_{max}, ensuring a broad exploration of possible α values. We adopt log-space sampling to generate these scale factors, $\{\alpha_1, \cdots, \alpha_n\}$, evenly on a logarithmic scale. In this case, these sampled scale factors can be denser in the smaller range, which is beneficial for the stable optimization process. We initiate the optimization with the smallest sampled scale factor to generate the initial optimized tree candidate. This candidate then serves as the starting point for the next optimization run with a slightly larger α. This iterative process is repeated until all sampled scale factors have been utilized. Detailed implementation steps are integrated within our systematic optimization framework, Algorithm 1.

D.1 Comparison between our annealing strategy and binary search for scale factor selections

Binary search provides a structured way to explore different α values for scaling the softmin approximation. Unlike random trials, it narrows the search range by evaluating performance at the midpoint and adjusting boundaries accordingly. While this is more principled than random guessing, it still involves testing isolated α values. As earlier discussed, this approach does not match the performance of our multi-run warm start annealing strategy.

While we agree that a binary search-like approach can be used to identify an effective α, our empirical results show that gradually increasing α, rather than directly using a large fixed value, leads to better training outcomes. This is because starting with a smaller α allows the model to optimize under a smoother case, improving stability. As α increases, it becomes sharper and closer to the ideal formulation, and the model benefits from being progressively adapted to this more accurate approximation. Our annealing strategy takes advantage of this effect by warm-starting each successive optimization task with the solution from previous task with smaller α. This gradual refinement enhances the approximation accuracy, while mitigating numerical instability typically associated with larger α.

The average training accuracy across Group **(i)** 17 regression datasets for different tree depths is summarized below. Our annealing strategy consistently outperforms binary search, with an average improvement of 2.82% across all depths.

Table 6: Training accuracy (optimization capability) comparison with different α selection strategies.

Tree Depth	2	4	8	12
Using Binary Search for α Selections	69.95	77.33	87.69	94.98
Using Our Multi-run Warm Start Annealing Strategy for α Selections	71.78	82.18	90.93	96.36

These results validate the effectiveness of our annealing in practice. However, we acknowledge that this finding is based on empirical observation, and a theoretical analysis is still lacking.

E An Illustrative Example of The Influence of Initial Solutions and Their Adjustments for Gradient-based Optimization

As discussed in Section 4.2, a good initial solution is crucial for achieving a better optimality, especially in our task with softmin operations. This is because our softmin operates on $U_{i,t}$, which is ReLU-based violations with either zero or non-zero values. However, these non-zero violations may be close to zero, especially for samples around the decision boundary $\boldsymbol{a}_j^T \boldsymbol{x}_i - b_j = 0$. While such small discrepancies between exact-zero and near-zero violation do not impact Argmin behaviors, which select the unique path only when $U_{i,t} = 0$, they can sensitively affect softmin. Specifically, softmin may fail to produce values close to one as ideally expected, potentially compromising approximation accuracy. Here, we provide an illustrative example to understand the influence of initial solutions and their adjustments for gradient-based optimization. As shown in Figure 3, the red sample x^* lies near the blue decision boundary, resulting in a small positive ReLU output, close to zero, that is difficult to distinguish from an exact zero.

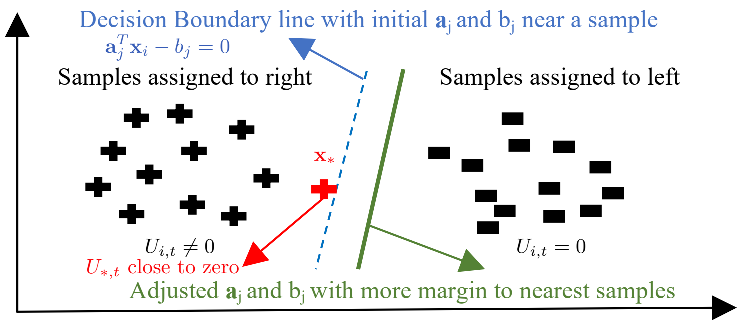
Decision Boundary line with initial $\mathbf{a}_j$ and b_j near a sample
$\mathbf{a}_j^T \mathbf{x}_i - b_j = 0$
Samples assigned to right
Samples assigned to left
$\mathbf{x}_*$
$U_{i,t} \neq 0$
$U_{*,t}$ close to zero
$U_{i,t} = 0$
Adjusted $\mathbf{a}_j$ and b_j with more margin to nearest samples

Figure 3: Illustration of the influence of initial solutions and the effective adjustments.

To mitigate this, the initial $\boldsymbol{A}$ and $\boldsymbol{b}$ can be adjusted so that the decision boundary achieves the maximum margin from the nearest samples, without altering the existing sample assignments as illustrated by the green line in Appendix E, Figure 3. This adjustment does not change sample assignments but enhances the distinction between exact-zero and near-zero cases.

The adjustment can be easily implemented either by calculating the median of $\boldsymbol{a}_j^T \boldsymbol{x}_i$ for the closest samples on both sides of the boundary, or using support vector machine to treat sample assignments as a binary classification task. To be more specific, Each branch test $\boldsymbol{a}_t^T \boldsymbol{x}_i \leq b_t$ acts as a binary classifier, directing samples left or right. A practical adjustment is to slightly shift the decision boundary (e.g., by modifying the median of $\boldsymbol{a}_j^T \boldsymbol{x}_i$) to enlarge the margin without changing sample assignments. Beyond only adjusting b_j, we also refine both $\boldsymbol{a}_j$ and b_j using an SVM: we treat left/right assignments as binary labels and fit a linear SVM to maximize margin. The resulting weights and bias update the split parameters while preserving the original assignment. This procedure is visualized in Appendix E, Figure 3.

F Hyperparameters Analysis of Our Differentiable Decision Tree Optimization Approach

Despite the introduction of additional hyperparameters in gradient-based optimization, tuning them is not typically necessary because their effects are straightforward. To be more specific, the hyperparameters in our differentiable decision tree optimization approach are as follows:

(1) The multi-start number N_{start}

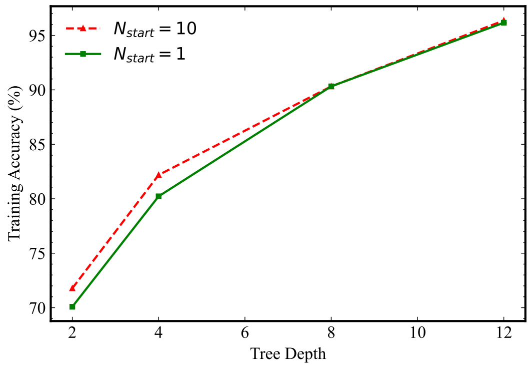

Figure 4: The trend of training optimality under different depth setting with different N_{start}.

The multi-start number N_{start} directly influences training optimality by increasing the chance of finding the optimal solution, albeit at a higher computational cost. In practice, N_{start} is set to balance acceptable computational expenses with desired training accuracy.

To explore the correlation between N_{start} and the training optimality, our "ReLU+Argmin"-based Differentiable Decision Tree Optimization (`RADDT`) for regression trees with constant predictions is performed under different N_{start} values as shown in Figure 4. It indicates that increasing N_{start} generally improves training optimality for all various tree depths, especially at lower tree depths.

(2) The epoch number N_{epoch}

The epoch number N_{epoch} is another hyperparameter that directly affects training optimality. A higher N_{epoch} value increases training accuracy, but it also increases computational costs. In practice, N_{epoch} is also set to balance acceptable computational expenses with desired training accuracy.

Our experiment with different $N_{epoch} = \{100, 3000, 5000\}$ in Figure 5, shows that increasing N_{epoch} generally improves training optimality for all various tree depths.

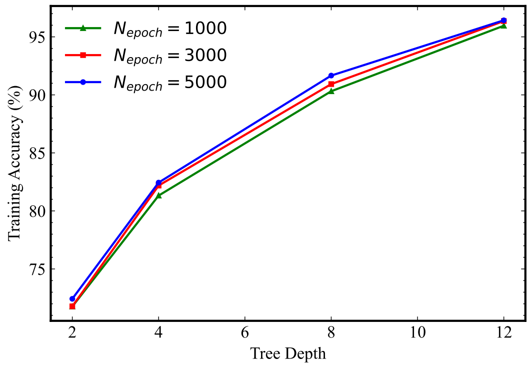

Figure 5: The trend of training optimality under different depth setting with various N_{epoch}.

(3) The range of sampled scale factors $[\alpha_{min}, \alpha_{max}]$ for scaled softmin function

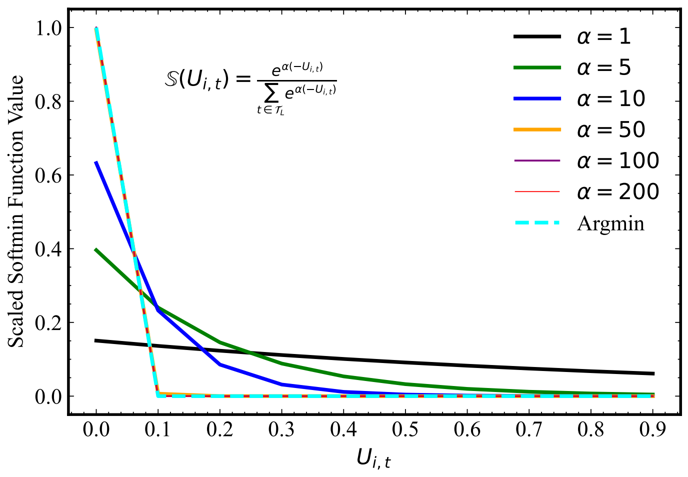

Figure 6: Comparison of scaled softmin function approximating Argmin behaviors under varying α.

This predetermined range is used to sample a set of scaled factors α for the strategy of multi-run warm start annealing. The principal aim is to explore a broader range of scale factors, ranging from smaller to larger values. As discussed in Section 3.2, the scaled softmin function applied to $U_{i,t}$ is used to approximate the Argmin function (more concretely, the one-hot encoded Argmin function). A larger α leads to a closer approximation to the Argmin function. As observed in Figure 6, the gap between scaled softmin function and the Argmin function narrows as α increases. Noticeably, the standard softmin function with $\alpha = 1$ exhibits a significant deviation from the Argmin function as depicted in the black line. With a larger α, such as $\alpha \geq 50$, the scaled softmin function closely approximates the Argmin function, almost overlapping with the Argmin function as shown in the figure. In the implementation of our experiments, we simply sample α within the range $[\alpha_{min}, \alpha_{max}] = [2, 200]$ to meet our requirements. This range ensures that smaller values maintain a smooth gradient and exhibit a better approximation than the standard softmin function, while larger values closely approximate the Argmin function.

(4) The number of sampled scale factors

Within a predetermined range, a set of scaled factors, denoted as $\{\alpha_1, \cdots, \alpha_n\}$, are sampled for subsequent use in multi-run warm start annealing, as detailed in Section 4.1. Larger scale factors reduce the approximation disparity, whereas smaller ones yield a smoother and more stable gradient. Including a greater number of scale factors in the set facilitates a more stable approximation process, enhancing the approximation degree to Argmin behaviors while minimizing the loss of differentiability typically associated with larger scale factors. Intuitively, including more scale factors in the set enhances training optimality. However, this leads to increased iterations in the annealing strategy, thereby raising computational costs. Practically, the number of scale factors is often determined by balancing training accuracy against computational demands. In our experiments, to avoid excessive computational costs, we primarily sample 5 scale factors with a log-space distribution within the range $[\alpha_{min}, \alpha_{max}]$.

(5) The learning rate η

The learning rate is a common parameter in gradient-based optimization, and has garnered significant attention in the literature. To simplify its usage, we adopt the well-established learning rate scheduler, termed `CosineAnnealingWarmRestarts` (with initial linear warm up) in PyTorch, which decreases the learning rate from an initial value of 0.01, thus minimizing the need for additional tuning.

G Algorithm Details of "ReLU+Argmin"-based Differentiable Decision Tree

Alongside the detailed descriptions in Section 4.3, we present the algorithmic implementation of our "ReLU+Argmin"-based Differentiable Decision Tree Optimization framework, `RADDT`, in Algorithm 1.

Algorithm 1 The entire tree optimization framework for RADDT.

```
1: Input: ${\boldsymbol{x}_i, y_i}_{i=1}^n$, tree depth $D$, learning rate $\eta$, epoch number $N_{epoch}$, multi-start number $N_{start}$.
2: Output: Optimal trainable variables $\boldsymbol{A}_{best}$, $\boldsymbol{b}_{best}$, $\theta_{best}$.
3: Define $\mathcal{L}_{min}$, empty variables $\boldsymbol{A}_{best}$, $\boldsymbol{b}_{best}$ and $\theta_{best}$.
4: for $start = 1$ to $N_{start}$ do
5:     Initialize $\boldsymbol{A}$, $\boldsymbol{b}$, $\theta$ with initial solution adjustments as detailed in Section 4.2. Generate scale factors
       $\{\alpha_1, \cdots, \alpha_n\}$ with log-spacing.
6:     for $\alpha_{iter} \in \{\alpha_1, \cdots, \alpha_n\}$ do
7:         If $iter \neq 1$, initialize trainable variables with the solution of last optimization run by Line 12.
8:         for $k = 1$ to $N_{epoch}$ do
9:             Calculate loss $\mathcal{L}$ at step $k$ by Equation (7) and calculate $\frac{\partial \mathcal{L}}{\partial \boldsymbol{A}}$, $\frac{\partial \mathcal{L}}{\partial \boldsymbol{b}}$, $\frac{\partial \mathcal{L}}{\partial \theta}$. Then update trainable
               variables via gradient decent, such as $\boldsymbol{A}_{k+1} = \boldsymbol{A}_k - \eta \frac{\partial \mathcal{L}}{\partial \boldsymbol{A}}$.
10:        end for
11:        Deterministically update $\theta$ without any approximation, as described in Appendix C.
12:        Generate a tree candidate with optimized variables, termed as $\boldsymbol{A}_{iter}$, $\boldsymbol{b}_{iter}$, $\theta_{iter}$. Specifically,
           $\boldsymbol{A}_{iter} = \boldsymbol{A}_{N_{epoch}}$ and $\boldsymbol{b}_{iter} = \boldsymbol{b}_{N_{epoch}}$, while $\theta_{iter}$ is derived through a deterministic recalculation
           as mentioned in Line 11.
13:        Deterministically compute $\mathcal{L}$ by Equation (5). IF $\mathcal{L} < \mathcal{L}_{min}$, update variables like $\boldsymbol{A}_{best} \leftarrow \boldsymbol{A}_{iter}$.
14:    end for
15: end for
```

H Detailed Description and Usage of The Four Groups of Datasets

Dataset split ratio and usage

In our experiments, typically, we allocate 75% of the samples for training purposes and the remaining 25% for testing, following the train-test split ratio as used in [Bertsimas and Dunn, 2017]. If an experiment requires cross validation for hyperparameter tuning like tree depth, we then subdivide the training datasets into training and validation subsets in a 2:1 ratio. The dataset setting accordingly changes to 50% samples as training set, 25% samples as validation set, and 25% samples as testing set. After determining the best hyperparameters, we then retrain the model using the combined training and validation set, and use the remaining 25% as the testing set to evaluate the final testing accuracy.

Dataset information across four groups

As discussed in Section 5, our baseline comparison experiments are conducted across four groups of datasets: **(i)** 17 medium-sized regression datasets with fewer than 41k samples (primary focus); **(ii)** 27 same classification and 9 regression datasets used in certain baselines (for more credible comparison on their used datasets); **(iii)** 4 real-world datasets with about 100 samples, and 3 synthetic datasets with 5000 samples (for comparing global optimality with global tree ORT-MIP [Bertsimas and Dunn, 2017] and known ground truth, respectively); **(iv)** 7 large-scale datasets with at least 1 million samples (for scalability).

Unless otherwise specified, these real-world datasets used for our regression experiments are collected from the UCI repository [Dua and Graff, 2019] and OpenML [Vanschoren et al., 2014]. Regarding the 17 medium-sized datasets in Group **(i)**, detailed information about these datasets is summarized in Table 7. The dataset size n and the number of features p are provided in the table.

Regarding the same classification datasets used in the original GradTree study [Karthikeyan et al., 2022] in Group **(ii)**, we include these shared datasets to support a more credible and convincing comparison. Although we have already compared against GradTree on the Group **(i)** 17 regression datasets in Table 7, and their subpar performance aligns with the results reported in their own Table 1 and 2, where their method underperforms the foundational baseline CART on 17 out of 36 classification datasets, we still further evaluate on the same classification datasets used in their own work to provide a more credible comparison. Among their 36 classification datasets, we finally collect 27 and discard 9 datasets, due to one or more of the following issues: unavailable dataset sources, unusable datasets with substantial missing values (corrupted dataset), or ambiguous dataset documentation. For example, the "rice" dataset lacks a clear download source. The "annealing" dataset contains a significantly large number of missing values and is nearly unusable. The "splice" dataset lacks clear information, such as the definition of features and predictive target, making this type of dataset unusable. Therefore, to ensure experimental reproducibility and data integrity, we

Table 7: Group (i) 17 real-world regression datasets from UCI and OpenML Repository.

Dataset Index	Dataset Name	Dataset Size (n)	Feature Number (p)
1	airfoil-self-noise	1,503	5
2	space-ga	3,107	6
3	abalone	4,177	8
4	gas-turbine-co-emission-2015	7,384	9
5	gas-turbine-nox-emission-2015	7,384	9
6	puma8NH	8,192	8
7	cpu-act	8,192	21
8	cpu-small	8,192	12
9	kin8nm	8,192	8
10	delta-elevators	9,517	6
11	combined-cycle-power-plant	9,568	4
12	electrical-grid-stability	10,000	12
13	condition-based-maintenance_compressor	11,934	16
14	condition-based-maintenance_turbine	11,934	16
15	ailerons	13,750	40
16	elevators	16,599	18
17	friedman-artificial	40,768	10

discard 9 datasets in total and perform the same-dataset comparison on the remaining 27 datasets. Additionally, since their work adopts a 20% test split, different from our default setting, we adopt their train-test split ratio for this specific comparison to ensure fairness. The final list of datasets, along with their sample size n, number of features p, and number of classes c, is presented in Table 8.

Table 8: Group (ii) 27 same classification datasets used in the original `GradTree` study.

Dataset Index	Dataset Name	Dataset Size (n)	Feature Number (p)	Class Number (c)
GradTree-1	balance-scale	625	4	3
GradTree-2	banknote-authentication	1,372	4	2
GradTree-3	blood-transfusion	748	4	2
GradTree-4	car-evaluation	1,728	6	4
GradTree-5	congressional-voting-records	232	16	2
GradTree-6	contraceptive-method-choice	1,473	9	3
GradTree-7	dermatology	358	34	6
GradTree-8	echocardiogram	61	11	2
GradTree-9	iris	150	4	3
GradTree-10	spambase	4,601	57	2
GradTree-11	thyroid-disease-ann-thyroid	7,200	21	3
GradTree-12	wine	178	13	3
GradTree-13	adult	32,561	14	2
GradTree-14	bank-marketing	45,211	14	2
GradTree-15	credit-card	30,000	23	2
GradTree-16	german	1,000	20	2
GradTree-17	glass	214	9	6
GradTree-18	heart-failure	299	12	2
GradTree-19	landsat	6,435	36	6
GradTree-20	loan-house	614	11	2
GradTree-21	lymphography	148	18	4
GradTree-22	mushrooms	8,124	22	2
GradTree-23	raisins	900	7	2
GradTree-24	segment	2,310	19	7
GradTree-25	solar-flare	1,389	10	8
GradTree-26	wisconsin-breast-cancer	569	10	2
GradTree-27	zoo	101	16	7

Regarding the same regression datasets used in the work of soft decision trees, no tabular datasets were used in [Frosst and Hinton, 2017], but we adopt the four tabular regression datasets from the original soft decision tree study by [İrsoy et al., 2012]. We include these shared datasets to support a more credible and convincing comparison as well. The shared 4 datasets are given in Table 9.

Regarding the same regression datasets used in `DTSemNet`, `DGT-Linear` and `TAO-Linear`, we also include these 5 shared datasets. We follow the same comparison setting and experimental setup as `DTSemNet` to include these 5 shared datasets for a more credible comparison against `DTSemNet`, `DGT-Linear` and `TAO-Linear`. Details of the shared 5 datasets are provided in Table 10.

For comparison of training optimality in Section 5.2, four small regression datasets with around 100 samples are also used. These datasets, collected from UCI and listed in Table 11, allow us to compare the training optimality of our method against global optimal solutions. The global optimal method `ORT-MIP` is computationally solvable for such a small dataset size as observed in our experiments.

Besides, three two-dimensional synthetic regression datasets with 5000 samples each are also used to showcase the effectiveness of our tree optimization in approaching global training optimality. Synthetic datasets are advantageous as they hold a known ground truth. Based on tree-based decision rules with the form of `IF-THEN` statements, we design 2^D decision rules to create a dataset by the D-depth tree. These decision rules are used to assign samples to the corresponding leaf nodes along a sequence of branching tests. For instance, when generating a two-dimensional dataset for a 2-depth tree, one of the decision rules is described as `IF` $x_{i,1} + x_{i,2} > 0$ `and` $x_{i,1} - x_{i,2} > 0$, `THEN` $y_i = 0.5$. In this setting, we generate 3 synthetic datasets, termed "Syn-2", "Syn-3" and "Syn-4" . These datasets are created with varying tree depth settings of 2, 3, and 4, respectively.

Table 9: Group (ii) 4 regression datasets used in original work of soft trees [İrsoy et al., 2012].

Dataset Index	Dataset Name	Dataset Size (n)	Feature Number (p)
SoftTree-1	abalone	4,177	8
SoftTree-2	puma8NH	8,192	8
SoftTree-3	computer	209	7
SoftTree-4	concrete	103	7

Table 10: Group (ii) five shared regression datasets used in original work of `DTSemNet`, `DGT` and `TAO`.

Dataset Index	Dataset Name	Dataset Size (n)	Feature Number (p)
DTSemNet-1	Abalone	4,177	8
DTSemNet-2	Comp-Active	8,192	21
DTSemNet-3	Ailerons	14,308	40
DTSemNet-4	CTSlice	53,500	384
DTSemNet-5	YearPred	515,345	90

Table 11: Group (iii) four small real-world regression datasets with about 100 samples.

Dataset Index	Dataset Name	Dataset Size (n)	Feature Number (p)
Small-1	concrete-slump-test-compressive	103	7
Small-2	concrete-slump-test-flow	103	7
Small-3	hybrid-price	153	4
Small-4	lpga-2008	157	6

Regarding the 7 large-scale regression datasets each with at least 1,000,000 samples in Group **(iv)**, they are used to evaluate the scalability of our method. These datasets are listed in Table 12. The dataset size n and the number of features p are provided in the table.

Table 12: Group (iv) seven large-scale regression datasets each with at least 1 million samples.

Dataset Index	Dataset Name	Dataset Size (n)	Feature Number (p)
Million-1	BNG-Ailerons	1,000,000	40
Million-2	BNG-cpu-act	1,000,000	21
Million-3	BNG-cpu-small	1,000,000	12
Million-4	BNG-puma32H	1,000,000	32
Million-5	BNG-wisconsin	1,000,000	32
Million-6	ACSPublicCoverage2018	1,138,289	19
Million-7	BNG-elevator	1,000,000	18

I The implementation Settings for Comparison Studies

To implement our "ReLU+Argmin"-based Differentiable Decision Tree optimization framework (`RADDT`), we utilize PyTorch that embeds auto differentiation tools and gradient-based optimizers. Our method is configured with $N_{epoch} = 3,000$ and $N_{start} = 10$, unless otherwise specified.

For benchmarking, the `Scikit-learn` library in `Python` is used to implement `CART` and random forest (`RF`) methods. `XGBoost` is implemented via their official package. The parameter values for these methods are set to default values, unless otherwise specified, such as the specific hyperparameters tuning for RF and XGBoost discussed in Section 5.1 and Appendix J. The implementation of HHCART, RandCART and OC1 is adapted from publicly sourced GitHub repository and programmed in Python. We modified their classification-oriented loss functions to adapt for regression tasks.

As for the local search method ORT-LS, we reproduce it in Julia due to the absence of open-source code for ORT-LS. Aiming to provide a reference for global training optimality, we also implement the MIP-based optimal oblique decision tree, ORT-MIP, in Julia, solving the MIP problem with Gurobi due to the absence of open-source code for ORT-MIP.

The GradTree, SoftDT, DGT and LatenTree methods are implemented using their respective open-source GitHub repositories, with adjustments made only to the epoch numbers to align with our methods. The TEL is implemented using their open-source code with their own default parameter settings, except for the number of trees and epoch numbers. We modify the epoch number to align with our experimental setup. Since it is a tree ensemble method, we set the number of trees to 10.

Since no open-source code is available for TAO-Linear, and the DTSemNet work directly uses the reported results from TAO-linear for comparison, we adopt the same approach to ensure consistency and credibility. DTSemNet itself is a decision tree with linear predictions. For consistency, it also adapts the original DGT tree with constant predictions into a linear variant, termed DGT-Linear. The datasets used in TAO-Linear are shared with DTSemNet and DGT-Linear, and DTSemNet directly collects the reported results from each method for comparison. Following their experimental setup, we apply the same data preprocessing, dataset splits and evaluation metric to implement our method on these five shared datasets. This allows for a fair and direct comparison between our results and the summarized benchmarks presented in DTSemNet' Table 4, covering DGT-Linear, TAO-Linear, and DTSemNet itself. Detailed implementation settings for these baselines can be found in DTSemNet Panda et al. [2024]. It is important to note that this, same-dataset comparison against TAO-Linear, DGT-Linear and DTSemNet, is the only experiment in which we directly adopt the reported results for DGT (DGT-Linear). In our other experiments involving DGT, including Table 3 in Section 5.2 and Table 22 in Appendix K.10, we implement the experiments using their open-source code software.

Experiments necessitating CPU computation were executed on the HPC Cluster, specifically utilizing "Dell EMC R440 CPU" configuration. Each CPU job is allocated 32G memory with a Time Limit of 7 days. Experiments for ORT-MIP requiring larger memory resources were carried out on the Oracle HPC Cluster, specifically with 2T memory and 128 cores. Concurrently, experiments requiring GPU resources were conducted on the "Narval" server, with an NVIDIA A100 GPU equipped.

J Hyperparameters Tuning for Tree Ensemble Methods

For a fair comparison, comprehensive hyperparameter tuning is also performed for three tree ensemble methods. Regarding random forest RF, the number of trees in a forest is a critical parameter. It is well-recognized that testing performance improves with an increase in the number of trees; however, the marginal gains become less pronounced as additional trees are added [Oshiro et al., 2012, Probst et al., 2019]. Accordingly, the number of trees is tuned across a set of $\{50, 100, 200, 300, 400, 500\}$. Moreover, the maximum tree depth is tuned over a broader range, from 1 to 50, to potentially capture optimal depth settings, given that RF empirically benefits from overly-deeper trees for enhanced testing accuracy. Other hyperparameters, including the number of features per split and the number of samples per tree, are maintained at default settings. These have been shown to balance the bias-variance trade-off, typically yielding robust performance with default values [Probst et al., 2019].

For XGBoost, we follow the same hyperparameter tuning schemes, varying the number of trees across a set $\{50, 100, 200, 300, 400, 500\}$, and the maximum tree depth from 1 to 50.

For the gradient-based tree ensemble TEL, no specific hyperparameter tuning is performed; we directly fix the number of trees to 10 and retain all other parameters at their default settings.

While our current hyperparameter tuning for tree ensembles, including those in Appendix K.6 with more-combination search for hyperparameters, is sufficient to support our main claims, especially given that our goal is not to claim superiority over ensembles, more tuning on regularization parameters could potentially yield even better results for tree ensembles.

K The Complementary Results of Numerical Experiments

K.1 Detailed testing accuracy comparison results on 17 medium-sized datasets in Group (i).

The testing accuracy (R^2) comparison for various decision trees on specific 17 medium-sized datasets in Group (i) is detailed in Table 13.

Table 13: Testing accuracy comparison for diverse decision trees on Group (i) 17 real-world datasets.

Datasets	Greedy methods				Gradient-based		Heurisitc Local Search	Our Optimized Tree	
	`CART`	`OC1`	`RandCART`	`HHCART`	`GradTree`	`SoftDT`	`ORT-LS`	`RADDT`	`RADDT-Linear`
1	85.27	86.38	76.79	85.71	56.46	67.06	85.24	90.34	90.65
2	42.14	40.53	50.70	49.05	30.47	47.46	49.51	59.46	61.20
3	47.29	46.15	46.94	54.75	49.68	55.28	54.20	57.03	58.74
4	66.50	55.39	57.24	60.61	64.07	60.80	55.62	62.19	71.62
5	82.19	83.20	83.30	84.43	67.03	80.81	86.39	89.63	88.59
6	62.36	62.71	41.64	66.95	61.53	60.31	63.68	65.21	68.11
7	96.98	97.23	92.06	97.15	95.30	85.36	97.59	97.47	98.25
8	95.89	96.25	95.78	96.25	93.69	88.66	96.65	96.26	97.31
9	42.56	51.53	51.83	56.32	44.22	71.60	69.57	81.26	86.23
10	60.19	59.03	58.42	60.91	54.76	62.76	58.52	61.86	63.58
11	93.33	93.15	93.11	93.55	84.66	93.16	92.84	94.00	94.22
12	71.17	74.72	58.08	68.80	45.01	86.35	80.66	87.22	91.74
13	98.58	94.37	98.45	98.63	85.17	86.83	98.93	97.76	99.99
14	97.34	71.14	96.11	95.23	76.81	48.37	97.78	96.30	99.97
15	75.96	76.55	75.48	77.92	67.49	81.61	78.44	81.46	82.42
16	69.12	72.30	65.03	75.66	49.73	86.57	82.61	89.61	90.57
17	85.51	85.69	69.52	82.75	67.03	73.33	89.18	93.51	95.49

The testing accuracy (R^2) comparison for 3 tree ensembles on specific 17 medium-sized datasets in Group (i) is detailed in Table 14.

Table 14: Testing accuracy comparison for three tree ensembles on Group (i) 17 real-world datasets.

Dataset Index	`RF`	`XGBoost`	`TEL`
1	92.58	93.39	88.76
2	53.22	53.84	69.79
3	57.64	57.40	61.23
4	68.10	65.55	56.55
5	91.00	90.78	88.11
6	68.38	66.79	67.00
7	98.27	98.54	97.78
8	97.63	97.72	97.35
9	70.48	75.29	90.57
10	63.16	64.15	62.31
11	95.92	96.49	94.01
12	89.59	92.80	95.30
13	99.50	99.51	98.31
14	98.74	98.67	92.37
15	83.24	83.39	81.76
16	83.59	90.01	89.88
17	93.41	95.36	94.70

K.2 Implementation details of same-dataset comparisons for certain baselines

For `GradTree`, we follow their experimental setup: using 20% of the data for testing, macro F1-score as evaluation metric, and averaging results over 10 runs with different random splits. Despite adhering to their dataset settings and hyperparameter configurations, we were unable to reproduce their reported results from Tables 1 and 2 in their paper. Therefore, we directly compare our `RADDT` results with their published results.

Regarding soft decision tree, no tabular datasets were used in [Frosst and Hinton, 2017], but we adopt the four tabular regression datasets from the original Soft Decision Tree study by [İrsoy et al., 2012]. As no specific dataset settings are provided in that work, we use our default experimental setup for both Soft Decision Tree and `RADDT`.

Regarding `TAO-Linear`, `DGT-Linear` and `DTSemNet`, since no open-source code is available for `TAO-Linear`, and the `DTSemNet` work directly uses the reported results from `TAO-Linear` for comparison, we adopt the same approach to ensure consistency and credibility. `DTSemNet` itself is a decisoin tree with linear predictions. For consistency, it also adapts the original DGT tree with constant predictions to a linear variant, referred to as DGT-Linear. Following DTSemNet's experimental setup, we apply the same data preprocessing, dataset splits (40% of the data for testing, unless otherwise specified for certain dataset) and evaluation metric (RMSE) to implement our method on the five shared datasets. This allows for a fair and direct comparison between our results and the summarized benchmarks presented in DTSemNet'Table 4, covering DGT-Linear, TAO- Linear, and DTSemNet itself. Detailed implementation settings for these baselines can be found in DTSemNet.

K.3 Detailed results for same-dataset comparison on Group (ii) 27 datasets used by GradTree

Our same-dataset comparison for GradTree is performed on 27 of their original 36 datasets, with 9 excluded due to unavailability or ambiguity. Detailed dataset information is given in Appendix H. The result for each dataset is given in Table 15, using macro F1-score as the evaluation metric, following their original study. Our method outperforms GradTree by 4.99% on average in test performance.

Table 15: Testing comparison on 27 shared classification datasets in Group (ii) with GradTree

Dataset Index	Dataset Name	Originally Reported Results in GradTree	Our RADDT
GradTree-1	balance-scale	59.30	90.10
GradTree-2	banknote-authentication	98.70	99.70
GradTree-3	blood-transfusion	62.80	66.00
GradTree-4	car-evaluation	44.00	86.80
GradTree-5	congressional-voting-records	95.00	96.60
GradTree-6	contraceptive-method-choice	49.60	48.40
GradTree-7	dermatology	93.00	94.40
GradTree-8	echocardiogram	65.80	83.30
GradTree-9	iris	93.80	95.10
GradTree-10	spambase	90.30	92.10
GradTree-11	thyroid-disease-ann-thyroid	90.50	95.80
GradTree-12	wine	93.30	97.80
GradTree-13	adult	74.30	76.40
GradTree-14	bank-marketing	64.00	71.90
GradTree-15	credit-card	67.40	68.20
GradTree-16	german	59.20	66.10
GradTree-17	glass	56.00	58.20
GradTree-18	heart-failure	75.00	75.80
GradTree-19	landsat	80.70	86.30
GradTree-20	loan-house	71.40	73.20
GradTree-21	lymphography	61.00	61.20
GradTree-22	mushrooms	100.00	100.00
GradTree-23	raisins	84.00	85.10
GradTree-24	segment	94.10	88.80
GradTree-25	solar-flare	15.10	15.40
GradTree-26	wisconsin-breast-cancer	90.40	94.80
GradTree-27	zoo	87.40	83.30

K.4 Detailed results for same-dataset comparison on Group (ii) 4 datasets used by soft trees

We provide the comparison results for each dataset in Table 16. The results show that RADDT outperforms the soft decision tree by 6.88% in testing accuracy (R^2), again aligning with prior results.

Table 16: Testing comparison on 4 shared regression datasets in Group (ii) with Soft Decision Tree

Dataset Index	Dataset Name	Soft Decision Tree	Our RADDT
SoftTree-1	abalone	55.28	57.03
SoftTree-2	puma8NH	60.31	65.21
SoftTree-3	computer	57.01	56.69
SoftTree-4	concrete	25.93	47.10

K.5 Detailed results for same-dataset comparison on Group (ii) 5 datasets used by DGT-Linear, TAO-Linear and DTSemNet

As earlier discussed in Section 5.1, we have compared our method with DGT-Linear, TAO-Linear and DTSemNet on the five shared datasets as used in the original work of DTSemNet. We extend DTSemNet's Table 4 by including our results under the same experimental setup in Table 17.

Table 17: Comparison on Group (ii) five datasets used by TAO-Linear, DGT-Linear and DTSemNet

Datasets	Our RADDT-Linear [1]		DTSemNet [2]		DGT-Linear [2]		TAO-Linear [2]	
	RMSE	Rank	RMSE	Rank	RMSE	Rank	RMSE	Rank
Abalone	**1.984**	**1**	2.135	3	2.144	4	2.07	2
Comp-Active	**2.519**	**1**	2.645	3	2.645	3	2.58	2
Ailerons	**1.154**	**1**	1.66	2	1.67	3	1.74	4
CTSlice	**1.138**	**1**	1.45	3	1.78	4	1.16	2
YearPred	11.934	4	**8.99**	**1**	9.02	2	9.08	3

[1] Following DTSemNet work, trees with linear prediction are compared. [2] These results are taken directly from DTSemNet's Table 4.

K.6 More extensive hyperparameter tuning for tree ensembles on Group (i) datasets

As previously indicated in Table 2, the findings of our methods being comparable to tree ensembles RF and XGBoost are based on 300-combination specific hyperparameter tuning scheme. In that setting, our method is tuned only over tree depths from 1 to 12 with 12 combinations, ensuring a much lighter tuning for fairness.

To further support this finding, we extend the parameter search space to 5,400 combinations. This involves tuning the "tree depth" within a range of {1-50, 55, 60, 70, 80, 90, 100, 150, 200, 250, 300}, "the number of trees" within {5, 10, 50, 100, 200, 300, 400, 500, 600, 700}, and with the additional tuning for RF on "the minimum samples per leaf and per split" in {1, 2, 4}, and for XGBoost on "subsample" and "colsample_bytree" in {0.6, 0.8, 1.0}. Additionally, to provide even stronger evidence, we further use PyCaret automated machine learning tool to perform an extensive 10,000-combination hyperparameter tuning for XGBoost, exploring its whole hyperparameter space with PyCaret's default search settings.

As shown in Table 18, the 5,400-combination tuning yields slight improvements in testing accuracy for both RF and XGBoost, with 0.11% gain for RF and 0.26% gain for XGBoost over the 300-combination tuning in Table 2. The extensive 10,000-combination tuning for XGBoost via PyCaret leads to just a 1.04% gain. Despite extensive tuning, our key finding remains consistent: our single tree achieves accuracy comparable to ensemble methods. Notably, our aim is not to claim superiority over tree ensembles, as any base learner including decision tree can be improved via ensemble techniques. Comparing a single tree to tree ensembles is inherently unfair. Instead, our goal is to showcase the potential of a single, optimized tree like ours in achieving high testing accuracy.

Table 18: Accuracy comparison on Group (i) datasets with extensive tuning for tree ensembles.

The Number of Hyperparameter Tuning Combinations	Testing Accuracy (R^2, %)
RF (300-combination reported in Table 2)	82.62
RF (5400-combination)	82.73
XGBoost (300-combination reported in Table 2)	83.51
XGBoost (5400-combination)	83.77
XGBoost (10000-combination by PyCaret)	84.55

K.7 Detailed comparison against optimal trees on 4 small datasets in Group (iii)

As earlier discussed, ORT-MIP [Bertsimas and Dunn, 2017] is computationally infeasible for previously-used datasets, even with 128 cores and a two-day time limit. It can only solve the 2-depth tree training problem on 4 small datasets in Group (iii) to a global optimum with 1% gap. Due to these limitations, only 50% samples are used for training in this experiment. Detailed training accuracy comparisons against ORT-MIP on these 4 small datasets are presented in Table 19.

Table 19: Train accuracy comparison results on solvable 4 small datasets in Group (iii).

Dataset	Sample	Feature	ORT-MIP	RADDT
concrete-slump-test-compressive	103	7	87.79	87.12
concrete-slump-test-flow	103	7	89.89	84.92
hybrid-price	153	4	78.09	73.50
lpga-2008	157	6	86.79	85.73
Average Training Accuracy (R^2, %)			85.64	82.82

Regarding the optimal sparse trees [Zhang et al., 2023], it complements earlier work on optimal trees (ORT-MIP) that fails to consider sparsity. As for experimental comparisons, optimal sparse trees may not be directly comparable to our method. First, optimal sparse trees are limited to axis-aligned splits, which generally yield lower accuracy than oblique trees. Second, they are designed for binary features, requiring feature discretization that may degrade performance on our continuous-feature datasets. We therefore choose not to include this in our experiments, as it could unfairly disadvantage their method under our evaluation setting.

K.8 Detailed comparisons against known ground truth on 3 synthetic datasets in Group (iii)

We provide the detailed comparison results for each synthetic dataset in Table 20. The known ground truths for both train and test accuracy are 100%. The results show that our `RADDT` closely approximate global optimality in train and test accuracy, with 0.64% difference over ground truth on average. These results, together with previous global solution comparisons, further validate the effectiveness of our tree optimization.

Table 20: Training and Testing performance on synthetic datasets in Group (iii).

Dataset	Fitted Depth		Training Accuracy (R^2, %)		Testing Accuracy (R^2, %)	
	`Ground-truth`	`RADDT`	`Ground-truth`	`RADDT`	`Ground-truth`	`RADDT`
Syn-2	2	2	100	99.96	100	99.99
Syn-3	3	3	100	98.78	100	98.71
Syn-4	4	4	100	99.35	100	99.39

K.9 Ablation experiments on the strategies used in our tree optimization

The observed superiority in training accuracy of our `RADDT` method can be attributed to two key strategies designed to enhance approximation accuracy, as discussed in Section 4: the multi-run warm start annealing strategy, and the strategy of adjusting initial solution for gradient-based optimization. The comparative results, presented in Table 21, clearly illustrate the impact of these strategies on `RADDT`. It should be noted that our method, which utilizes the multi-run warm start annealing, is referred to as `RADDT` in the table. In contrast, when this strategy is not employed, the method is denoted by specific values of scale factors, such as $\alpha = 1$ and $\alpha = 150$. Additionally, the strategy of adjusting initial solutions is evaluated in the table, with the method labeled as `RADDT` without adjustments to initial solution and `RADDT` with adjustments to initial solution.

Regarding multi-run warm start annealing, we analyze training accuracy with and without this strategy. Without this strategy, we utilize fixed scale factors for comparison: a standard softmin function with a small $\alpha = 1$, and a larger scale factor $\alpha = 150$. The findings indicate substantial improvements with the annealing approach: training accuracy increased by 9.7%, 9.32%, 8.46% and 1.07% at tree depths of 2, 4, 8, and 12, respectively, when compared to the standard softmin function without any scaling. Moreover, when compared to fixed scale factors larger than 1, the annealing strategy also yields a higher training accuracy. These results confirm that our multi-run warm start annealing strategy is effective in enhancing training accuracy, by striking a greater balance between the approximation accuracy of scaled softmin function and the stability of gradient-based optimization.

The strategy of adjusting the initial solution for gradient-based optimization also contributes to these improvements. It boosts training accuracy by 1.3%, 2.89%, 1.01% and 1.84% at tree depths of 2, 4, 8, and 12, respectively. Notably, these gains are achieved solely through improved initialization, without involving in the optimization process.

Table 21: The effectiveness of strategies used in our tree optimization approach on training accuracy.

Item		$D=2$	$D=4$	$D=8$	$D=12$
without Multi-run Warm Start Annealing (A fixed Scale Factor)	$\alpha = 1$ (Standard Softmin Function)	60.78	69.97	81.46	93.45
	$\alpha = 150$	68.00	78.31	88.08	94.42
with Multi-run Warm Start Annealing (Our `RADDT` method)	`RADDT` without adjustments to initial solution	70.48	79.29	89.92	94.52
	`RADDT` with adjustments to initial solution	71.78	82.18	90.93	96.36

K.10 Scalability comparison on 7 million-scale datasets in Group (iv)

In Section 5.3, we analyze the scalability of various methods on 7 million-scale datasets in Group (iv) under a fixed-depth setting. The detailed results are presented in Table 22.

Table 22: Scalability comparison under fixed-depth setting on 7 million-scale datasets in Group (iv).

Methods[1]	Training Accuracy (R^2, %)				Testing Accuracy (R^2, %)				Training Time (s)			
	D2	D4	D8	D12	D2	D4	D8	D12	D2	D4	D8	D12
`CART`	24.18	35.19	42.06	47.80	23.91	34.99	41.35	41.57	6	9	17	25
`RandCART`	17.17	22.71	28.35	33.22	17.11	22.57	27.98	29.78	9	16	38	67
`HHCART`	22.40	27.20	36.40	42.29	22.29	27.07	36.03	38.79	12	24	46	84
`GradTree`	19.67	26.92	33.36	/	19.48	26.60	33.16	/	1,387	3,058	14,570	/
`SoftDT`	18.19	27.36	28.36	/	18.13	27.24	28.21	/	29	136	16,263	/
`DGT`	30.26	35.27	/	/	30.10	34.99	/	/	202,537	232,574	/	/
`LatentTree`	33.35	40.04	/	/	33.00	39.74	/	/	73,965	72,130	/	/
`RADDT`	33.93	39.39	43.56	51.67	33.56	39.01	42.27	39.59	8,136	5,596	21,874	80,731

[1] `OC1` and `ORT-LS` fail even at depth 2 within 14 days. `GradTree`, `SoftDT`, `DGT`, and `LatentTree` face out-of-memory issues when scaling, with `GradTree` and `SoftDT` failing at depth 12, and `DGT` and `LatentTree` only solvable at depths 2 and 4.

K.11 GPU-accelerated implementation for our `RADDT` experiments

Our differentiable tree is trained by solving an unconstrained optimization problem, offering substantial scalability benefits via its reformulated structure. Furthermore, by leveraging mature frameworks like PyTorch, our implementation facilitates GPU acceleration, including distributed data parallel with multi-GPU. Under ideal full GPU utilization, training can also be distributed across multiple GPUs, further reducing time in proportion to the number of GPUs used. Concerning the training time reported in Table 3, our `RADDT` method achieves superior accuracy without a substantial increase in training time. While single-GPU acceleration is enabled for both our `RADDT` and other compared gradient-based trees, Our `RADDT` attains more efficient acceleration by fully leveraging matrix operation in computing our designed loss in Equation (7), which integrates unique tree path formulation. Specifically, by introducing the parameter $U_{i,t}$, we store the deterministic sample route and assignments in a matrix to avoid loop-based calculation at every iteration, enabling efficient matrix operations for loss and gradient calculations. Additionally, for training 12-depth trees on Group (i) datasets with more than 10,000 samples, we use 4 GPUs to further accelerate our `RADDT`.

Regarding scalability experiments on million-scale datasets reported in Table 22, we utilize 4 GPUs to train our `RADDT` at depths 2, 4, and 8, and 8 GPUs for depth 12. This distributed data parallelism is easily implemented using our extensible framework, which supports multi-GPU training through simple commands without requiring any specialized parallelization design.

K.12 Training time and speedup analysis on Group (i) datasets with over 10,000 samples

As in Table 3, our `RADDT` achieves superior accuracy without substantial increase in training time compared to other trees, such as the second-best `ORT-LS`. These scalability advantages become more pronounced when dealing with larger matrix operations, particularly involving in deeper trees or larger datasets with more samples and feature dimensions. To illustrate this, we provide a detailed comparison of training time and speedup for 12-depth tree training between `RADDT` and `ORT-LS` on the datasets with more than 10,000 samples in Group (i). The results are summarized in Table 23.

Table 23: The speedup of `RADDT` over `ORT-LS` for 12-depth tree training on Group (i) datasets with more than 10,000 samples.

Dataset Index	Dataset Name	Dataset Size (n)	Feature Number (p)	`ORT-LS` (Time, s)	`RADDT` (Time, s)	Speedup (`ORT-LS/RADDT`)
12	electrical-grid-stability	10,000	12	197,361.31	1,691.10	116.71
13	condition-based-maintenance_compressor	11,934	16	232,929.77	2,036.77	114.36
14	condition-based-maintenance_turbine	11,934	16	251,017.34	2,026.15	123.89
15	ailerons	13,750	40	965,968.22	2,236.61	431.89
16	elevators	16,599	18	485,509.64	2,622.17	185.16
17	friedman-artificial	40,768	10	671,460.77	4,331.58	155.02

K.13 Comparison of our method's training time in GPU versus CPU settings

In this section, we provide a comparison of our method's training time in GPU versus CPU settings, although the advantages of GPU acceleration are expected. We use a fixed dataset, "sgemm-product", with subsets varying sizes from {100, 1,000, 5,000, 10,000, 50,000} for training 8-depth and 12-depth trees. As expected, GPU training is significantly faster. For instance, on 50,000 samples with an 8-depth tree, GPU training is 117 times faster than CPU. For a 12-depth tree on 1,000 samples, we observe a 107 times speed-up. On larger datasets and deeper trees, the CPU version often fails to complete within 5 days. This highlights the practical importance of GPU acceleration for scalability.

Table 24: Training time comparison of our RADDT method in GPU versus CPU settings.

	Training Time (Second)			
	8-depth treee		12-depth tree	
Datasize	One GPU	CPU	One GPU	CPU
100	337	615	769	10,912
1,000	359	2,938	1,043	111,111
5,000	466	22,082	2,799	OOT >5 days
10,000	614	46,132	5,057	OOT >5 days
50,000	2,949	345,992	41,564	OOT >5 days

Additionally, as discussed in Appendix K.10, Appendix K.11 and Appendix K.12, also observed in this comparison, the GPU advantages become increasingly pronounced with larger matrix operations, particularly involving deeper trees, larger datasets with more samples and feature dimensions.

K.14 Interpretability analysis of our optimized tree

We fully agree that orthogonal trees like CART are more interpretable at the same, fixed depth. However, as originally discussed in OC1 [Murthy et al., 1994], oblique trees can become more interpretable when they require substantially less depth.

Our RADDT's interpretability can be assessed from three aspects: tree-based prediction logic, unique prediction path and the complexity of decision rules. First, RF, in Table 2, using an average of 314.71 trees for higher accuracy, almost losing the interpretability for final predictions compared to a single tree. Second, our tree with ReLU-based hard splits maintains a unique decision path leading to final predictions. These hard splits preserve the interpretability of True-False decision-making, which is often compromised in soft trees with a probabilistic path. Third, regarding the complexity of decision rules, oblique trees tend to generate smaller trees with clear oblique decision boundaries compared to orthogonal trees like CART. For example, using synthetic dataset "Syn-4" in Table 20, CART achieves only 85.27% training accuracy for a 4-depth tree, whereas our RADDT attains 99.35% for the same depth. To achieve a comparable train accuracy, CART requires a deeper 9-depth tree with accuracy reaching to 99.88%. Detailed results of CART under various depths are given in Table 25. CART with 9-depth tree results in a complex, staircased boundary, shown in Figure 7. Such complexity can make decision rules difficult to interpret, whereas oblique trees with simpler and fewer splitting rules. It makes our RADDT more interpretable despite the use of 2-feature combinations in tree splits. Notably, this example does not imply oblique tree holds better interpretability, but rather to exhibit exclusive interpretability in certain datasets where underlying data distribution align with oblique boundaries.

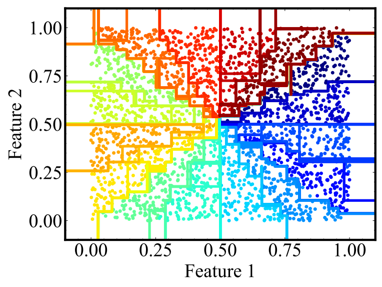

(a) by 9-depth CART

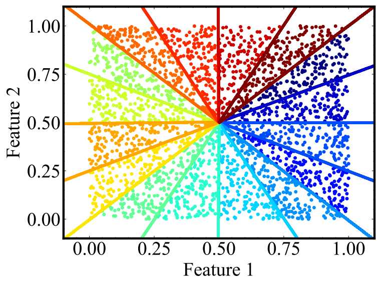

(b) by 4-depth RADDT

Figure 7: The decision boundary comparison for dataset "Syn-4".

Table 25: Train and Test accuracy for CART on synthetic dataset "Syn-4" under various tree depths.

Item	Various Tree Depth									
	1	2	3	4	5	6	7	8	9	10
Training Accuracy (R^2, %)	27.65	56.86	73.39	85.27	92.41	96.49	98.20	99.61	99.88	99.96
Testing Accuracy (R^2, %)	25.91	54.23	71.67	80.65	84.36	87.04	87.93	87.83	87.75	88.19

When compared to other oblique trees as reported in Table 1 and Table 2, our methods achieve superior accuracy but also with a lower depth, such as our RADDT with depth of 7.29 and RADDT-Linear with depth of 4.82. This reduction in depth significantly enhances interpretability with fewer rules. To illustrate, a 2-depth tree yields 4 decision rules across 2 layers, whereas a 10-depth tree produces 1024 rules across 10 layers. Understanding hundreds of nested IF-THEN rules can be challenging.

Additionally, as in Table 4, our methods can achieve slightly better accuracy than CART with significantly smaller trees: average depths of 2.82 (RADDT) and 1 (RADDT-Linear), compared to 10.24 for CART, leading to 30-80 times fewer parameters. In this case, for example, 1-depth tree consists of only 2 leaf nodes with 2 rules, which is highly interpretable because we can explain model predictions as "IF the feature combination is less than a threshold, THEN the prediction is based on the left leaf node; otherwise, right leaf node." These results highlight oblique tree's advantages in higher accuracy with smaller depth, typically yielding less prediction rules and fewer model parameters.

Therefore, interpretability depends on multiple factors including tree depth, feature number, and the accuracy-simplicity trade-off. There is no interpretability superiority of one approach over the other, as it depends on specific application scenarios.

K.15 Overfitting issue and comparison for trees with linear predictions

As discussed in Section 5.6, overfitting issues have been observed with both our RADDT and RADDT-Linear method. Upon further comparison of our RADDT-Linear with the existing open-source library linear-tree, it is evident that the overfitting issues are more pronounced in trees with linear predictions. The open-source software linear-tree exhibits significantly more severe overfitting issues at depths such as 8 and 12, as detailed in Table 26.

For our RADDT-Linear, although the training accuracy improves by 6.52% from depth 4 to 8, testing accuracy conversely drops by 9.67%, indicating a serious overfitting issue. To mitigate the overfitting issues for RADDT-Linear, we preliminarily attempt to apply L_1 regularization to trainable variables $\boldsymbol{A}$. This approach involves incorporating a regularization term into the loss function $\mathcal{L}$ below, serving to penalize the complexity of the tree structure. The regularized loss is delineated in Equation (8), where λ denotes the regularization strength and $\|\cdot\|_1$ represents the L_1 norm.

However, identifying the appropriate regularization strength λ proves to be challenging during our experiments, necessitating extensive hyperparameter tuning. This tuning significantly increases the computational cost and the implementation complexity of our method. Consequently, in our experiment reported in Table 2, we did not tune this parameter. We just use a very small value $1e-4$ to implement a minimal regularization, aiming to enhance testing accuracy without greatly compromising the optimization capabilities. With this slight regularization, the testing accuracy of RADDT-Linear reported in Table 2 is improved by 0.58% compared to the results without regularization, as shown in Table 27. Despite the slight improvement, the overfitting issues for RADDT-Linear still exist, and our preliminary regularization is not sufficient to address this issue. Significant improvements in testing accuracy are achievable through appropriate regularization strategies; however, this requires further exploration and is limited in this paper.

Table 26: Comparison of training and testing accuracy for RADDT-Linear and linear-tree.

Depth	Training Accuracy (R^2, %)		Testing Accuracy (R^2, %)	
	linear-tree	RADDT-Linear	linear-tree	RADDT-Linear
2	79.85	82.92	79.46	81.74
4	85.47	86.73	73.58	83.10
8	93.33	93.25	-376648.84 (overfitting)	73.43
12	98.31	98.00	-11288345.94 (overfitting)	38.98

$$\mathcal{L}_{reg} = \sum_{i=1}^{n} \sum_{t \in \mathbb{T}_L} \mathbb{S}\left(U_{i,t}\right) \left(y_i - \left(\boldsymbol{k}_t^T \boldsymbol{x}_i + h_t\right)\right)^2 + \lambda \sum_{t \in \mathbb{T}_b} \|\boldsymbol{a}_t\|_1 \tag{8}$$

Table 27: The comparison for RADDT-Linear with and without regularization across 17 datasets.

Item	RADDT-Linear without regularization	RADDT-Linear with regularization
Testing Accuracy (R^2, %)	84.05	84.63

NeurIPS Paper Checklist

1. **Claims**

   Question: Do the main claims made in the abstract and introduction accurately reflect the paper's contributions and scope?

   Answer: [Yes]

   Justification: The main claims in the abstract and introduction accurately reflect the paper's contributions, including the proposal of a novel decision tree formulation with demonstrated accuracy and scalability benefits, as supported by our experimental results.

   Guidelines:

   - The answer NA means that the abstract and introduction do not include the claims made in the paper.
   - The abstract and/or introduction should clearly state the claims made, including the contributions made in the paper and important assumptions and limitations. A No or NA answer to this question will not be perceived well by the reviewers.
   - The claims made should match theoretical and experimental results, and reflect how much the results can be expected to generalize to other settings.
   - It is fine to include aspirational goals as motivation as long as it is clear that these goals are not attained by the paper.

2. **Limitations**

   Question: Does the paper discuss the limitations of the work performed by the authors?

   Answer: [Yes]

   Justification: The limitations of our work are explicitly discussed in Section 5.6, with experimental discussions in Appendix K.15.

   Guidelines:

   - The answer NA means that the paper has no limitation while the answer No means that the paper has limitations, but those are not discussed in the paper.
   - The authors are encouraged to create a separate "Limitations" section in their paper.
   - The paper should point out any strong assumptions and how robust the results are to violations of these assumptions (e.g., independence assumptions, noiseless settings, model well-specification, asymptotic approximations only holding locally). The authors should reflect on how these assumptions might be violated in practice and what the implications would be.
   - The authors should reflect on the scope of the claims made, e.g., if the approach was only tested on a few datasets or with a few runs. In general, empirical results often depend on implicit assumptions, which should be articulated.
   - The authors should reflect on the factors that influence the performance of the approach. For example, a facial recognition algorithm may perform poorly when image resolution is low or images are taken in low lighting. Or a speech-to-text system might not be used reliably to provide closed captions for online lectures because it fails to handle technical jargon.
   - The authors should discuss the computational efficiency of the proposed algorithms and how they scale with dataset size.
   - If applicable, the authors should discuss possible limitations of their approach to address problems of privacy and fairness.
   - While the authors might fear that complete honesty about limitations might be used by reviewers as grounds for rejection, a worse outcome might be that reviewers discover limitations that aren't acknowledged in the paper. The authors should use their best judgment and recognize that individual actions in favor of transparency play an important role in developing norms that preserve the integrity of the community. Reviewers will be specifically instructed to not penalize honesty concerning limitations.

3. **Theory assumptions and proofs**

   Question: For each theoretical result, does the paper provide the full set of assumptions and a complete (and correct) proof?

Answer: [NA]

Justification: This work does not include theoretical proofs and results.

Guidelines:

- The answer NA means that the paper does not include theoretical results.
- All the theorems, formulas, and proofs in the paper should be numbered and cross-referenced.
- All assumptions should be clearly stated or referenced in the statement of any theorems.
- The proofs can either appear in the main paper or the supplemental material, but if they appear in the supplemental material, the authors are encouraged to provide a short proof sketch to provide intuition.
- Inversely, any informal proof provided in the core of the paper should be complemented by formal proofs provided in appendix or supplemental material.
- Theorems and Lemmas that the proof relies upon should be properly referenced.

4. **Experimental result reproducibility**

   Question: Does the paper fully disclose all the information needed to reproduce the main experimental results of the paper to the extent that it affects the main claims and/or conclusions of the paper (regardless of whether the code and data are provided or not)?

   Answer: [Yes]

   Justification: We provide full details of our model architecture with a novel decision tree reformulation in Section 3, training procedures in Algorithm 1, hyperparameters analysis in Appendix F, and evaluation metrics. The datasets used are publicly available detailed in Appendix H, and reproduction scripts are provided in a GitHub repository. Together, these materials ensure that experimental results can be reproduced.

   Guidelines:

   - The answer NA means that the paper does not include experiments.
   - If the paper includes experiments, a No answer to this question will not be perceived well by the reviewers: Making the paper reproducible is important, regardless of whether the code and data are provided or not.
   - If the contribution is a dataset and/or model, the authors should describe the steps taken to make their results reproducible or verifiable.
   - Depending on the contribution, reproducibility can be accomplished in various ways. For example, if the contribution is a novel architecture, describing the architecture fully might suffice, or if the contribution is a specific model and empirical evaluation, it may be necessary to either make it possible for others to replicate the model with the same dataset, or provide access to the model. In general. releasing code and data is often one good way to accomplish this, but reproducibility can also be provided via detailed instructions for how to replicate the results, access to a hosted model (e.g., in the case of a large language model), releasing of a model checkpoint, or other means that are appropriate to the research performed.
   - While NeurIPS does not require releasing code, the conference does require all submissions to provide some reasonable avenue for reproducibility, which may depend on the nature of the contribution. For example
     (a) If the contribution is primarily a new algorithm, the paper should make it clear how to reproduce that algorithm.
     (b) If the contribution is primarily a new model architecture, the paper should describe the architecture clearly and fully.
     (c) If the contribution is a new model (e.g., a large language model), then there should either be a way to access this model for reproducing the results or a way to reproduce the model (e.g., with an open-source dataset or instructions for how to construct the dataset).
     (d) We recognize that reproducibility may be tricky in some cases, in which case authors are welcome to describe the particular way they provide for reproducibility. In the case of closed-source models, it may be that access to the model is limited in some way (e.g., to registered users), but it should be possible for other researchers to have some path to reproducing or verifying the results.

5. **Open access to data and code**

   Question: Does the paper provide open access to the data and code, with sufficient instructions to faithfully reproduce the main experimental results, as described in supplemental material?

   Answer: [Yes]

   Justification: The datasets used are publicly available from UCI and OpenML, as detailed in Appendix H. We provide open access to the source code of our method via a GitHub repository, along with detailed instructions to run the code and reproduce the main experimental results.

   Guidelines:

   - The answer NA means that paper does not include experiments requiring code.
   - Please see the NeurIPS code and data submission guidelines (`https://nips.cc/public/guides/CodeSubmissionPolicy`) for more details.
   - While we encourage the release of code and data, we understand that this might not be possible, so "No" is an acceptable answer. Papers cannot be rejected simply for not including code, unless this is central to the contribution (e.g., for a new open-source benchmark).
   - The instructions should contain the exact command and environment needed to run to reproduce the results. See the NeurIPS code and data submission guidelines (`https://nips.cc/public/guides/CodeSubmissionPolicy`) for more details.
   - The authors should provide instructions on data access and preparation, including how to access the raw data, preprocessed data, intermediate data, and generated data, etc.
   - The authors should provide scripts to reproduce all experimental results for the new proposed method and baselines. If only a subset of experiments are reproducible, they should state which ones are omitted from the script and why.
   - At submission time, to preserve anonymity, the authors should release anonymized versions (if applicable).
   - Providing as much information as possible in supplemental material (appended to the paper) is recommended, but including URLs to data and code is permitted.

6. **Experimental setting/details**

   Question: Does the paper specify all the training and test details (e.g., data splits, hyperparameters, how they were chosen, type of optimizer, etc.) necessary to understand the results?

   Answer: [Yes]

   Justification: All experimental settings are clearly specified in the paper. Dataset usage, data splits and hyperparameter selections are described in in Appendix H and Appendix F. Detailed experimental procedures and algorithm configurations are also provided in Appendix I, ensuring the results can be fully understood and interpreted.

   Guidelines:

   - The answer NA means that the paper does not include experiments.
   - The experimental setting should be presented in the core of the paper to a level of detail that is necessary to appreciate the results and make sense of them.
   - The full details can be provided either with the code, in appendix, or as supplemental material.

7. **Experiment statistical significance**

   Question: Does the paper report error bars suitably and correctly defined or other appropriate information about the statistical significance of the experiments?

   Answer: [Yes]

   Justification: In addition to reporting performance metrics in comparison tables, we conduct paired T-tests to assess the statistical significance of our results. This analysis provides further support for the validity of our comparisons, as given in Section 5.1.

Guidelines:

- The answer NA means that the paper does not include experiments.
- The authors should answer "Yes" if the results are accompanied by error bars, confidence intervals, or statistical significance tests, at least for the experiments that support the main claims of the paper.
- The factors of variability that the error bars are capturing should be clearly stated (for example, train/test split, initialization, random drawing of some parameter, or overall run with given experimental conditions).
- The method for calculating the error bars should be explained (closed form formula, call to a library function, bootstrap, etc.)
- The assumptions made should be given (e.g., Normally distributed errors).
- It should be clear whether the error bar is the standard deviation or the standard error of the mean.
- It is OK to report 1-sigma error bars, but one should state it. The authors should preferably report a 2-sigma error bar than state that they have a 96% CI, if the hypothesis of Normality of errors is not verified.
- For asymmetric distributions, the authors should be careful not to show in tables or figures symmetric error bars that would yield results that are out of range (e.g. negative error rates).
- If error bars are reported in tables or plots, The authors should explain in the text how they were calculated and reference the corresponding figures or tables in the text.

8. **Experiments compute resources**

   Question: For each experiment, does the paper provide sufficient information on the computer resources (type of compute workers, memory, time of execution) needed to reproduce the experiments?

   Answer: [Yes]

   Justification: We provide detailed information about the compute resources used for our experiments, as detailed in Appendix I.

   Guidelines:

   - The answer NA means that the paper does not include experiments.
   - The paper should indicate the type of compute workers CPU or GPU, internal cluster, or cloud provider, including relevant memory and storage.
   - The paper should provide the amount of compute required for each of the individual experimental runs as well as estimate the total compute.
   - The paper should disclose whether the full research project required more compute than the experiments reported in the paper (e.g., preliminary or failed experiments that didn't make it into the paper).

9. **Code of ethics**

   Question: Does the research conducted in the paper conform, in every respect, with the NeurIPS Code of Ethics `https://neurips.cc/public/EthicsGuidelines`?

   Answer: [Yes]

   Justification: We have reviewed the NeurIPS Code of Ethics and confirm that our research fully complies with its principles.

   Guidelines:

   - The answer NA means that the authors have not reviewed the NeurIPS Code of Ethics.
   - If the authors answer No, they should explain the special circumstances that require a deviation from the Code of Ethics.
   - The authors should make sure to preserve anonymity (e.g., if there is a special consideration due to laws or regulations in their jurisdiction).

10. **Broader impacts**

    Question: Does the paper discuss both potential positive societal impacts and negative societal impacts of the work performed?

Answer: [NA]

Justification: This work focuses on foundational advances in differentiable decision tree learning and is not tied to any specific application with immediate societal impact.

Guidelines:

- The answer NA means that there is no societal impact of the work performed.
- If the authors answer NA or No, they should explain why their work has no societal impact or why the paper does not address societal impact.
- Examples of negative societal impacts include potential malicious or unintended uses (e.g., disinformation, generating fake profiles, surveillance), fairness considerations (e.g., deployment of technologies that could make decisions that unfairly impact specific groups), privacy considerations, and security considerations.
- The conference expects that many papers will be foundational research and not tied to particular applications, let alone deployments. However, if there is a direct path to any negative applications, the authors should point it out. For example, it is legitimate to point out that an improvement in the quality of generative models could be used to generate deepfakes for disinformation. On the other hand, it is not needed to point out that a generic algorithm for optimizing neural networks could enable people to train models that generate Deepfakes faster.
- The authors should consider possible harms that could arise when the technology is being used as intended and functioning correctly, harms that could arise when the technology is being used as intended but gives incorrect results, and harms following from (intentional or unintentional) misuse of the technology.
- If there are negative societal impacts, the authors could also discuss possible mitigation strategies (e.g., gated release of models, providing defenses in addition to attacks, mechanisms for monitoring misuse, mechanisms to monitor how a system learns from feedback over time, improving the efficiency and accessibility of ML).

11. **Safeguards**

    Question: Does the paper describe safeguards that have been put in place for responsible release of data or models that have a high risk for misuse (e.g., pretrained language models, image generators, or scraped datasets)?

    Answer: [NA]

    Justification: This work does not involve models or datasets with high risk of misuse, and thus no specific safeguards are necessary.

    Guidelines:

    - The answer NA means that the paper poses no such risks.
    - Released models that have a high risk for misuse or dual-use should be released with necessary safeguards to allow for controlled use of the model, for example by requiring that users adhere to usage guidelines or restrictions to access the model or implementing safety filters.
    - Datasets that have been scraped from the Internet could pose safety risks. The authors should describe how they avoided releasing unsafe images.
    - We recognize that providing effective safeguards is challenging, and many papers do not require this, but we encourage authors to take this into account and make a best faith effort.

12. **Licenses for existing assets**

    Question: Are the creators or original owners of assets (e.g., code, data, models), used in the paper, properly credited and are the license and terms of use explicitly mentioned and properly respected?

    Answer: [Yes]

    Justification: The datasets used are clearly cited as originating from UCI and OpenML. All baseline code sources are properly credited and detailed in the paper.

    Guidelines:

    - The answer NA means that the paper does not use existing assets.

- The authors should cite the original paper that produced the code package or dataset.
- The authors should state which version of the asset is used and, if possible, include a URL.
- The name of the license (e.g., CC-BY 4.0) should be included for each asset.
- For scraped data from a particular source (e.g., website), the copyright and terms of service of that source should be provided.
- If assets are released, the license, copyright information, and terms of use in the package should be provided. For popular datasets, `paperswithcode.com/datasets` has curated licenses for some datasets. Their licensing guide can help determine the license of a dataset.
- For existing datasets that are re-packaged, both the original license and the license of the derived asset (if it has changed) should be provided.
- If this information is not available online, the authors are encouraged to reach out to the asset's creators.

13. **New assets**

    Question: Are new assets introduced in the paper well documented and is the documentation provided alongside the assets?

    Answer: [Yes]

    Justification: We release our reproduction code as a new asset under an open-source license via a GitHub repository. The code is well documented, with clear instructions and usage details provided.

    Guidelines:

    - The answer NA means that the paper does not release new assets.
    - Researchers should communicate the details of the dataset/code/model as part of their submissions via structured templates. This includes details about training, license, limitations, etc.
    - The paper should discuss whether and how consent was obtained from people whose asset is used.
    - At submission time, remember to anonymize your assets (if applicable). You can either create an anonymized URL or include an anonymized zip file.

14. **Crowdsourcing and research with human subjects**

    Question: For crowdsourcing experiments and research with human subjects, does the paper include the full text of instructions given to participants and screenshots, if applicable, as well as details about compensation (if any)?

    Answer: [NA]

    Justification: The work does not involve crowdsourcing nor research with human subjects.

    Guidelines:

    - The answer NA means that the paper does not involve crowdsourcing nor research with human subjects.
    - Including this information in the supplemental material is fine, but if the main contribution of the paper involves human subjects, then as much detail as possible should be included in the main paper.
    - According to the NeurIPS Code of Ethics, workers involved in data collection, curation, or other labor should be paid at least the minimum wage in the country of the data collector.

15. **Institutional review board (IRB) approvals or equivalent for research with human subjects**

    Question: Does the paper describe potential risks incurred by study participants, whether such risks were disclosed to the subjects, and whether Institutional Review Board (IRB) approvals (or an equivalent approval/review based on the requirements of your country or institution) were obtained?

    Answer: [NA]

Justification: The work does not involve crowdsourcing nor research with human subjects.

Guidelines:

- The answer NA means that the paper does not involve crowdsourcing nor research with human subjects.
- Depending on the country in which research is conducted, IRB approval (or equivalent) may be required for any human subjects research. If you obtained IRB approval, you should clearly state this in the paper.
- We recognize that the procedures for this may vary significantly between institutions and locations, and we expect authors to adhere to the NeurIPS Code of Ethics and the guidelines for their institution.
- For initial submissions, do not include any information that would break anonymity (if applicable), such as the institution conducting the review.

16. **Declaration of LLM usage**

Question: Does the paper describe the usage of LLMs if it is an important, original, or non-standard component of the core methods in this research? Note that if the LLM is used only for writing, editing, or formatting purposes and does not impact the core methodology, scientific rigorousness, or originality of the research, declaration is not required.

Answer: [NA]

Justification: The core method development in this research does not involve LLMs as any important, original, or non-standard components.

Guidelines:

- The answer NA means that the core method development in this research does not involve LLMs as any important, original, or non-standard components.
- Please refer to our LLM policy (`https://neurips.cc/Conferences/2025/LLM`) for what should or should not be described.